

Hadronic Light-by-light Scattering Contribution to Muon $g - 2$

M. Hayakawa^{1 *}, T. Kinoshita^{2 †}, and A. I. Sanda^{1 ‡}

¹ *Department of Physics, Nagoya University, Nagoya 464-01 Japan*

² *Newman Laboratory, Cornell University, Ithaca, New York 14853 USA*

(January 21, 1996)

Abstract

The hadronic light-by-light scattering contribution to muon $g - 2$ is examined based on the low energy effective theories of QCD, the Nambu-Jona-Lasinio model and hidden local symmetry approach, supplemented by a general information concerning the asymptotic behavior of QCD. Our result is -52×10^{-11} with an uncertainty of $\pm 18 \times 10^{-11}$, which includes our best estimate of model dependence. This is within the expected measurement uncertainty of 40×10^{-11} in the forthcoming experiment at Brookhaven National Laboratory. Our result removes one of the main theoretical obstacles in verifying the existence of the weak contribution to the muon $g - 2$.

PACS numbers: 13.40.Em, 11.15.Pg, 12.39.Fe, 14.60.Ef

Typeset using REVTeX

* Electronic address: hayakawa@eken.phys.nagoya-u.ac.jp

† Electronic address: tk@hepth.cornell.edu

‡ Electronic address: sanda@eken.phys.nagoya-u.ac.jp

I. INTRODUCTION

A substantial improvement in the measurement of the muon anomalous magnetic moment $a_\mu \equiv \frac{1}{2}(g_\mu - 2)$ is planned at the Brookhaven National Laboratory. The precision of the measurement is expected to reach the level of [1]

$$40 \times 10^{-11}. \tag{1.1}$$

This is about 20 times more accurate than the best value available at present [2]

$$a_\mu(\text{exp}) = 1\,165\,923(8.5) \times 10^{-9}, \tag{1.2}$$

where the numerals in the parentheses represent the uncertainties in the last digits of the measured value.

Compared with the electron anomaly, for which all contributions other than QED are negligible, the muon anomaly is more sensitive to shorter scales where the hadronic and weak interaction effects are important. Also, provided that the standard model prediction is known precisely, the muon anomaly will be a sensitive probe of physics beyond the standard model. A typical standard model prediction is [3]

$$a_\mu(\text{th}) = 116\,591\,877(176) \times 10^{-11}. \tag{1.3}$$

We note that the uncertainty in (1.3) is comparable with the one-loop weak interaction correction [4]

$$a_\mu(\text{weak-1}) = 195(1) \times 10^{-11}. \tag{1.4}$$

Thus further improvement of the theoretical prediction is necessary in order to be able to confirm the existence of the weak correction term in a_μ .

The uncertainty in (1.3) is dominated by the error associated with the estimate of the strong interaction correction to a_μ . The bulk of this effect is due to the hadronic vacuum polarization contribution, which starts at $\mathcal{O}(\alpha^2)$. (See Fig. 1 of Ref. [5] for the Feynman graphs which give this type of contribution.) Fortunately, this contribution is calculable

without relying on our theoretical knowledge of strong interaction. The $\mathcal{O}(\alpha^2)$ contribution to the $a_\mu(\text{had.v.p.})$ can be expressed in the form [6]

$$a_\mu(\text{had.v.p.})|_{\mathcal{O}(\alpha^2)} = \left(\frac{\alpha m_\mu}{3\pi}\right)^2 \int_{4m_\pi^2}^{\infty} ds \frac{R(s)K(s)}{s^2} \quad (1.5)$$

by applying the dispersion relation and the optical theorem. Here $R(s)$ is the hadron production cross section in e^+e^- collisions normalized to the lowest order formula for the $\mu^+\mu^-$ production cross section $\sigma(e^+e^- \rightarrow \mu^+\mu^-) = 4\pi\alpha^2/3s$. The formula (1.5) enables us to reduce the issue of our ignorance of strong interaction dynamics to the experimental determination of $R(s)$ [7]. The integral (1.5) has been evaluated by several groups [5,8,9]. For instance the estimate given in Ref. [3] is

$$a_\mu(\text{had.v.p.}) = 7\,068\,(59)\,(164) \times 10^{-11}, \quad (1.6)$$

where the first and second errors are statistical and systematic, respectively. Works [9,10] which include more recent data are not too far off from (1.6), although the evaluation of uncertainties in the experimental data still varies considerably among authors. Future measurements at VEPP-2M, DAΦNE, and BEPS are expected to reduce these uncertainties to the level of the upcoming experiment (1.1) [10,11].

On the other hand, the contribution of the hadronic light-by-light scattering diagram shown in Fig. 1 is potentially a source of more serious difficulty because it cannot be expressed in terms of experimentally accessible observables and hence must be evaluated by purely theoretical consideration. The purpose of this paper is to report on our attempt to estimate this hadronic light-by-light scattering contribution to the muon anomaly. A summary of our preliminary results has been given in Ref. [12]. We present the detailed analysis here.

The paper is organized as follows. Sec. II starts with a survey of previously reported results on the hadronic light-by-light scattering contribution to the muon $g-2$. With the help of chiral perturbation theory and Nambu-Jona-Lasinio (NJL) model, we find that the relevant diagrams associated with this contribution are the ones shown in Fig. 2 of Ref.

[13]. We also give an outline of strategies to solve the problems we have encountered. The next three sections are devoted to the treatment of the three types of diagrams; Sec. III to the charged pseudoscalar loop contribution of Fig. 2(a), Sec. IV to the neutral pseudoscalar pole contribution of Fig. 2(b), and Sec. V to the quark loop contribution of Fig. 2(c). Sec. VI summarizes the present study and compares it with the recent result of Ref. [14,15] based on the extended Nambu-Jona-Lasinio (ENJL) model and discuss its implications.

II. SURVEY AND IMPROVEMENTS

This section begins with an overview of the previous studies on the hadronic light-by-light scattering contribution to the muon anomaly. We then point out a few problems associated with its evaluation, and describe the procedure which we have adopted to solve them.

A. Previous Studies

The muon anomalous magnetic moment receives important contributions from hadronic physics. Naive dimensional consideration suggests that the effect of the physics of the typical scale Λ higher than the muon mass m_μ is suppressed by $(m_\mu/\Lambda)^2$. This implies that contributions to a_μ from QCD will be dominated by nonperturbative aspects of QCD. Thus we are confronted with a calculational difficulty; the relevant hadronic contribution to the light-by-light scattering amplitude may not be calculable from first principles in the current stage of development of QCD.

As the next best procedure, we may appeal to the chiral perturbation theory which attempts to describe the low energy dynamics of QCD in terms of hadrons. Its leading behavior is given unambiguously by the low energy theorems on the dynamics of pions (and kaons) which are the Nambu-Goldstone bosons resulting from spontaneous breakdown of chiral symmetry. The scalar QED calculation in Ref. [5] corresponds to the lowest-order evaluation in this context. Corrections to the lowest order results may be obtained by adding higher order terms of a power series expansion in momentum variables.

For the calculation of the muon $g - 2$, however, such a systematic chiral perturbation technique runs into some problems. Insertion of a vertex with high power of momentum into Feynman diagrams for the muon anomaly, as a correction to the hadronic light-by-light scattering amplitude, yields a divergent result. Thus we must resort to an alternative approach which unfortunately is more model-dependent. For instance, Ref. [5] introduced the vector meson resonances. It should be noted that the explicit incorporation of vector mesons allows one to compute higher order counterterms [16] in the chiral Lagrangian. The resulting $\mathcal{O}(p^4)$ counter terms agree reasonably well with experimental determination. A well-known example of the success in this direction can be seen in the description of pion's electromagnetic form factor $F(q^2)$, where q is the photon momentum. There, the vector meson dominance (VMD) model works even for q as large as the mass of ρ meson, $M_\rho \simeq 760$ MeV .

Now we shall return to our topic. From the point of view of chiral perturbation theory, pions will contribute to a_μ most significantly in the form of the diagrams shown in Fig. 2(a) and (b). A priori we do not know the magnitudes of photon momenta which are important for these contributions. For example one may attempt to estimate the contribution of Fig. 2(a) in the lowest-order of chiral expansion which we will denote as $a_\mu(a, \text{sQED})$. On the other hand we recognize that the VMD model describes the $\pi^+\pi^-\gamma$ coupling well for on-shell pions. Thus we are motivated to include the VMD model explicitly in the $\pi\pi\gamma$ coupling. A naive approach, which leads to $a_\mu(a, \text{nVMD})$, introduces vector meson to replace a photon propagator as [5] ;

$$\frac{i}{q^2} \rightarrow \frac{i}{q^2} \frac{M_\rho^2}{M_\rho^2 - q^2} = \frac{i}{q^2} - \frac{i}{M_\rho^2 - q^2} . \quad (2.1)$$

The numerical results obtained by following these procedures were [17]

$$\begin{aligned} a_\mu(a, \text{sQED}) &= -0.043\ 7\ (36) \times \left(\frac{\alpha}{\pi}\right)^3 \\ &= -54.76\ (46) \times 10^{-11}, \end{aligned} \quad (2.2)$$

and

$$\begin{aligned}
a_\mu(a, \text{nVMD}) &= -0.012\ 5\ (19) \times \left(\frac{\alpha}{\pi}\right)^3 \\
&= -15.67\ (2.38) \times 10^{-11},
\end{aligned}
\tag{2.3}$$

respectively. We see a large modification when vector mesons are introduced. A natural question arising from this observation is :

(Q_1) Is the modification caused by the introduction of VMD model real ? If it is, why it seems to conflict with our expectation based on chiral perturbation theory that the vector meson effect is very small at low energies ?

Next let us turn our attention to the diagram shown in Fig. 2(b). It includes the $\pi^0\gamma\gamma$ vertex induced by the chiral anomaly. It is well-known that the effective interaction

$$\mathcal{L} = -\frac{\alpha}{8\pi f_\pi} \pi^0 \epsilon^{\mu\nu\lambda\sigma} F_{\mu\nu} F_{\lambda\sigma},
\tag{2.4}$$

where $f_\pi \simeq 93\text{MeV}$ is the pion decay constant and $F_{\mu\nu}$ is the field strength of photon, describes the behavior of $\pi^0\gamma\gamma$ vertex in the limit of zero pion momentum and on-shell photons. However, naive use of Eq. (2.4) for the $\pi^0\gamma\gamma$ vertices in the diagram of Fig. 2(b) leads to an ultra-violet divergent result. This is a signal that the interaction (2.4) is not applicable to photons and pions far off mass-shell and must be replaced there by some form factor. In Ref. [5] such a form factor was introduced by an *ad hoc* adoption of the VMD picture. Correcting a sign error in the previous calculation [5], this contribution was found to be

$$\begin{aligned}
a_\mu(b) &= -0.044\ 36\ (2) \times \left(\frac{\alpha}{\pi}\right)^3 \\
&= -55.60\ (3) \times 10^{-11}.
\end{aligned}
\tag{2.5}$$

In the previous analysis the quark loop diagram in Fig. 2(c) has been treated as *not* independent of the first two diagrams. Rather it was used as an alternative approximation of the hadronic light-by-light scattering contribution to a_μ . If this assertion is correct, the result for quark loop [5]

$$\begin{aligned}
a_\mu(c) &= 0.048\ (3) \times \left(\frac{\alpha}{\pi}\right)^3, \\
&= 62\ (3) \times 10^{-11},
\end{aligned}
\tag{2.6}$$

in which constituent quark masses are used, should be nearly equal to the sum of (2.3) and (2.5). However, even their signs do not agree with each other.

Therefore there arises the second question:

(Q_2) Are three diagrams shown in Fig. 2 independent after all ?

We will examine these questions and explore the prescriptions for remedy in the next subsection.

B. Improvements

First consider the question Q_1 . It has been pointed out that the naive VMD model of [5] does not respect the Ward identities required from electromagnetic gauge symmetry [18]. We found further that it is not compatible with chiral symmetry. To solve these problems, it is useful to introduce VMD in a way that preserves chiral symmetry. This can be achieved by appealing to the hidden local symmetry (HLS) approach [19]. This formulation maintains gauge invariance and chiral symmetry explicitly and reproduces all the low energy theorems assured by chiral symmetry, such as the KSFR relation. The question Q_1 may thus be raised within the HLS framework. Keep in mind, however, that this approach is somewhat oversimplified. In particular it ignores higher resonances beyond the usual vector mesons. We must analyze and reevaluate the error in our final result taking account of the model-dependence.

We shall now turn to the second question Q_2 . The previous work assumed that the quark loop calculation and the pion calculation are two distinct approximations to the same hadronic light-by-light scattering effect on a_μ . They should, therefore, yield the similar results and must not be added together. As was noted in Ref. [13], however, in the extended Nambu-Jona-Lasinio (ENJL) model, the quark loop diagram contribution is independent of the other two so that all three contributions should be added altogether.

This point can be made clearer by considering the $1/N_c$ expansion together with the chiral expansion. Table I lists the orders of each diagram shown in Fig. 2. According to

the QCD-diagrammatic consideration, the pion loop needs at least two quark loops, and the pion pole diagram starts from a diagram in which at least one gluon propagates between a quark and an antiquark forming the pion. Thus a single quark loop contribution is not included in these two graphs.

We may also examine this problem from the viewpoint of duality. In a dispersion relation for the light-by-light scattering amplitude, the integral over the quark loop diagram, from threshold to very high energies, is equal to the integral over the absorptive part due to all the hadronic intermediate states. Extension of this relation to local duality implies that the quark loop contribution approximates the hadronic contribution when certain averaging over a finite energy region is taken. Thus one may wonder if the quark loop diagram Fig. 2(c), when embedded in the $g - 2$ graph, represents the entire hadronic contribution.

We do not think so for the following reason. Consider a similar problem in the photon vacuum polarization diagram, and look at the cross section for low energy reaction $e^+e^- \rightarrow \text{hadrons}$. Duality between the quark diagram and the resonances implies that

$$\int \sigma(e^+e^- \rightarrow \text{hadrons}; Q^2) dQ^2 \approx \int \sigma(e^+e^- \rightarrow q\bar{q}; Q^2) dQ^2 \quad (2.7)$$

where the integration range is sufficiently large so that the resonance is averaged out. In this sense, it is well known that the absorptive part of one quark loop diagram for the photon vacuum polarization is dual to the cross section from the $\pi\pi$ threshold to about 1 GeV. This region is dominated by the ρ meson intermediate state, and the quark loop represents this contribution. Then there is a small continuum $\pi\pi$ state contribution at lower energies. Near threshold, they can be calculated by chiral symmetry argument. Is this a part of the quark loop diagram or is it a non-resonating continuum? If it is a part of ρ , we suspect that a chiral invariant $\pi\pi$ interaction should be able to generate the ρ meson bound state. As is well known [20], however, the force between two π mesons is not attractive enough to generate a bound ρ state. This supports the view that the $\pi\pi$ intermediate state at low energies is independent of ρ resonance and hence independent of one-quark-loop contribution. For the photon vacuum polarization graph, pion loop graph and quark loop graph are independent

and must be added together.

The above argument suggests that the pion loop is independent of the quark loop in light-by-light scattering, too. The quark loop diagram corresponds to the sum of continuum hadronic channels as well as axial vector meson states. Of course, this is by no means a proof. Since it is impossible to prove this type of statements without solving QCD, we must keep this ambiguity in mind in our subsequent analysis.

Let us summarize the above considerations and add a few corollaries:

(1) The HLS approach avoids the inconsistency that has been observed in the naive VMD approach used in the previous analysis, i.e., violation of chiral symmetry and electromagnetic Ward identities (This will be demonstrated in Sec. III B).

(2) Three diagrams shown in Fig. 2 should be added. Especially the quark loop diagram which represents the averaged hadronic continuum effect in a certain energy region has been discussed as independent of the other two.

(3) Contributions involving more loops of hadrons will be suppressed by a factor $m_\mu/(4\pi f_\pi)$ compared to the contributions of Fig. 2(a) and Fig. 2(b). On the other hand, the η pole contribution from a diagrams similar to that of Fig. 2(b) may not be negligible. The magnitude of this contribution and the kaon loop contribution from diagrams similar to Fig. 2(a) deserves an explicit analysis.

(4) As was mentioned already, naive use of Eq. (2.4) for the $\pi^0\gamma\gamma$ vertices of Fig. 2(b) leads to ultra-violet divergence, indicating that (2.4) must be modified by a form factor far off mass-shell. Possible modification dictated by the asymptotic behavior of QCD will be discussed in Sec. VI. Here we simply note that the prescription adopted in Ref. [5], in which the VMD was introduced merely as a convenient UV cut-off, can be justified within the HLS approach [21]. Note that the HLS Lagrangian can be obtained as an effective theory of the ENJL model [22]. Thus, a similar conclusion can also be reached in the ENJL model - the pion pole diagram contains two triangle loops of constituent quarks and ρ mesons is allowed to propagate before the quarks couple to photons. Fig. 3 shows this contribution diagrammatically. However, its evaluation needs some care, especially due to

the requirement of anomalous Ward identities [14], as is described in Sec. IV B.

(5) In the quark loop diagram, the vector meson will affect the coupling of the quark to the photon. Using the ENJL model as a guide we determine the quark coupling to vector mesons. Its graphical expression is found in Fig. 4 of Ref. [13].

III. CHARGED PSEUDOSCALAR LOOP

A. Hidden Local Symmetry Approach

For a complete description of HLS, the reader is referred to Ref. [19]. Mainly for the purpose of giving the Feynman rule relevant to our problem, we shall briefly discuss the formalism. The HLS incorporates vector mesons, such as ρ , as gauge particles of HLS, $[SU(2)_V]_{\text{local}}$ in our case. The explicit form of the Lagrangian, assuming chiral symmetry $[SU(2)_L \times SU(2)_R]_{\text{global}}$ and hidden local symmetry $[SU(2)_V]_{\text{local}}$ is

$$\begin{aligned} \mathcal{L} = & -\frac{1}{2g_V^2} \text{Tr} (F_{V\mu\nu} F_V^{\mu\nu}) - \frac{1}{4} F_{\mu\nu} F^{\mu\nu} + \mathcal{L}_A + a\mathcal{L}_V \\ & + \frac{1}{2} f_\pi^2 B_0 \left\{ \text{Tr}(\xi_L \mathcal{M} \xi_R^\dagger) + \text{Tr}(\xi_R \mathcal{M}^\dagger \xi_L^\dagger) \right\} \end{aligned} \quad (3.1)$$

where

$$\begin{aligned} \mathcal{L}_A &= f_\pi^2 \text{Tr} \left((\hat{\alpha}_{\parallel}^\mu(x))^2 \right), \\ \mathcal{L}_V &= f_\pi^2 \text{Tr} \left((\hat{\alpha}_{\perp}^\mu(x))^2 \right). \end{aligned} \quad (3.2)$$

In Eq.(3.1) $F_{V\mu\nu}$ and $F_{\mu\nu}$ are the field strengths of the vector meson $V_\mu = g_V \frac{\tau^a}{2} V_\mu^a$ (τ^a , $a = 1, 2, 3$, are Pauli matrices) and the photon A_μ , respectively, and g_V represents the coupling constant associated with HLS. f_π is the pion decay constant (~ 93 MeV), and the coefficient a of \mathcal{L}_V is an arbitrary constant to be fixed by experiment. $\hat{\alpha}_{\{\parallel, \perp\}\mu}$ consists of covariant derivatives of the basic objects $\xi_L(x)$ and $\xi_R(x)$ in the HLS approach:

$$\begin{aligned} \hat{\alpha}_{\parallel\mu} &= \frac{D_\mu \xi_L \cdot \xi_L^\dagger + D_\mu \xi_R \cdot \xi_R^\dagger}{2i}, \\ \hat{\alpha}_{\perp\mu} &= \frac{D_\mu \xi_L \cdot \xi_L^\dagger - D_\mu \xi_R \cdot \xi_R^\dagger}{2i}, \end{aligned} \quad (3.3)$$

where the covariant derivatives $D_\mu \xi_{L,R}(x)$ are given by

$$D_\mu \xi_{L,R}(x) = \partial_\mu \xi_{L,R}(x) - iV_\mu(x)\xi_{L,R}(x) + ie\xi_{L,R}(x)\frac{\tau^3}{2}A_\mu(x). \quad (3.4)$$

ξ_L and ξ_R contain the pion field $\pi^a(x)$ as well as the scalar triplet $\sigma^a(x)$:

$$\begin{aligned} \xi_R(x) &= e^{i\sigma(x)/f_\pi} e^{i\pi(x)/f_\pi}, \\ \xi_L(x) &= e^{i\sigma(x)/f_\pi} e^{-i\pi(x)/f_\pi}, \end{aligned} \quad (3.5)$$

where $\pi(x) = \pi^a(x)\frac{\tau^a}{2}$ and $\sigma(x) = \sigma^a(x)\frac{\tau^a}{2}$. The latter, on breaking the symmetry, will be absorbed into vector mesons V_μ to give them masses. In the last term of Eq. (3.1) B_0 is a dimension-one constant associated with the quark condensate [23]

$$B_0 = -\frac{1}{f_\pi^2} \langle 0 | \bar{u}u | 0 \rangle. \quad (3.6)$$

It combines with the current quark mass m_u in the mass matrix $\mathcal{M} = \text{diag}(m_u, m_d)$ (we neglect the isospin violation due to the quark masses so that we set $m_d = m_u$ henceforth) to give the pion masses

$$m_{\pi^\pm}^2 = m_{\pi^0}^2 = 2B_0 m_u. \quad (3.7)$$

In the unitary gauge $\sigma = 0$ for HLS, the relevant interaction terms for the present computation can be found as follows:

$$\begin{aligned} \mathcal{L}_{\text{int}} &= -eg_\rho A^\mu \rho_\mu^0 - ig_{\rho\pi\pi} \rho_\mu^0 \pi^+ \overleftrightarrow{\partial}^\mu \pi^- - ig_{\gamma\pi\pi} A_\mu \pi^+ \overleftrightarrow{\partial}^\mu \pi^- \\ &+ (1-a)e^2 A^\mu A_\mu \pi^+ \pi^- + 2eg_{\rho\pi\pi} A^\mu \rho_\mu^0 \pi^+ \pi^-. \end{aligned} \quad (3.8)$$

In this expression various masses and coupling constants are related to each other by [19]

$$M_\rho^2 = ag_V^2 f_\pi^2, \quad (3.9)$$

$$g_\rho = ag_V f_\pi^2, \quad (3.10)$$

$$g_{\rho\pi\pi} = \frac{1}{2} ag_V, \quad (3.11)$$

$$g_{\gamma\pi\pi} = \left(1 - \frac{a}{2}\right) e, \quad (3.12)$$

and A_μ represents the photon field to the order e^2 . As is seen from Eq. (3.12) the complete vector meson dominance (namely $g_{\gamma\pi\pi} = 0$) is realized when $a = 2$. This is also close to the observed data. Note that Eq. (3.8) does not contain the $\rho^0\rho^0\pi^+\pi^-$ term. This is the crucial difference between the chiral Lagrangian (3.1) and the VMD model of Ref. [5]. The absence of $\pi^+\pi^-\rho^0\rho^0$ coupling with no derivatives will be a common feature of chiral symmetric effective model, as implied by other models, too [16,24].

B. Ward Identity

Einhorn argued [18] that the calculation of Ref. [5] does not satisfy the Ward identities among the couplings of π and γ required from the electromagnetic symmetry. The purpose of this subsection is to demonstrate its recovery in the present approach. For simplicity let us consider a $\pi\gamma$ scattering amplitude and show explicitly that the relevant Ward identity is satisfied in the present approach. If we define the amputated Green functions $G^{\mu\nu}$ and Γ^μ in momentum space by

$$\begin{aligned}
(2\pi)^4\delta^4(q-k+p_1-p_2)G^{\mu\nu}(q,k;p_1,p_2) &= \\
&\int d^4ze^{iq\cdot z}\int d^4xe^{-ik\cdot x}\int d^4y_1e^{ip_1\cdot y_1}\int d^4y_2e^{-ip_2\cdot y_2}\langle 0|T[j_{em}^\mu(z)A^\nu(x)\pi^+(y_1)\pi^-(y_2)]|0\rangle_{\text{amp.}}, \\
(2\pi)^4\delta^4(k-p_1+p_2)i\Gamma^\mu(k;p_1,p_2) &= \\
&= \int d^4xe^{-ik\cdot x}\int d^4y_1e^{ip_1\cdot y_1}\int d^4y_2e^{-ip_2\cdot y_2}\langle 0|T[A^\mu(x)\pi^+(y_1)\pi^-(y_2)]|0\rangle_{\text{amp.}}, \tag{3.13}
\end{aligned}$$

and denote the (full) pion propagator as $iD(p)$, the Ward identity can be written as

$$-q^\mu G_{\mu\nu}(q,k;p_1,p_2) = \frac{iD(p_1+q)}{iD(p_1)}\Gamma_\nu(k;p_1+q,p_2) - \frac{iD(p_2-q)}{iD(p_2)}\Gamma_\nu(k;p_1,p_2-q). \tag{3.14}$$

In the naive VMD model of Ref. [5] the photon propagator [25]

$$\frac{-i}{p^2}, \tag{3.15}$$

is replaced everywhere by

$$\frac{-i}{p^2} - \frac{-i}{p^2 - M_\rho^2} = i\frac{M_\rho^2}{p^2(p^2 - M_\rho^2)}. \tag{3.16}$$

Thus, in this VMD model, the Green function Γ_μ (or $G_{\mu\nu}$) defined above is simply obtained by the multiplication of one (or two) ρ propagator(s) to the corresponding quantity in scalar QED

$$\begin{aligned}
G_{\mu\nu}(q, k, p_1, p_2) &= -e \frac{M_\rho^2}{q^2 - M_\rho^2} \frac{M_\rho^2}{k^2 - M_\rho^2} \left[2g_{\mu\nu} - \frac{1}{(k + p_2)^2 - m_\pi^2} (2p_2 + k)_\nu (2p_1 + q)_\mu \right. \\
&\quad \left. - \frac{1}{(p_1 - k)^2 - m_\pi^2} (2p_1 - k)_\nu (2p_2 - q)_\mu \right], \\
\Gamma_\mu(k; p_1, p_2) &= e \frac{M_\rho^2}{M_\rho^2 - k^2} (p_1 + p_2)_\mu.
\end{aligned} \tag{3.17}$$

Evidently the identity (3.14) cannot hold due to the difference in the numbers of ρ propagators between Γ_μ and $G_{\mu\nu}$. On the other hand, in the HLS approach, they are given, to the order of our interest, by

$$\begin{aligned}
G_{\mu\nu}(q, k; p_1, p_2) &= -e \left[2 \left\{ g_{\mu\nu} - \frac{a}{2} H_{\mu\nu}(k) - \frac{a}{2} H_{\mu\nu}(q) \right\} \right. \\
&\quad - \frac{1}{(k + p_2)^2 - m_\pi^2} \left\{ g_{\nu\beta} - \frac{a}{2} H_{\nu\beta}(k) \right\} (2p_2 + k)^\beta \left\{ g_{\mu\alpha} - \frac{a}{2} H_{\mu\alpha}(q) \right\} (2p_1 + q)^\alpha \\
&\quad \left. - \frac{1}{(p_1 - k)^2 - m_\pi^2} \left\{ g_{\nu\beta} - \frac{a}{2} H_{\nu\beta}(k) \right\} (2p_1 - k)^\beta \left\{ g_{\mu\alpha} - \frac{a}{2} H_{\mu\alpha}(q) \right\} (2p_2 - q)^\alpha \right], \\
\Gamma_\mu(k; p_1, p_2) &= e \left(g_{\mu\beta} - \frac{a}{2} H_{\mu\beta}(k) \right) (p_1 + p_2)^\beta.
\end{aligned} \tag{3.18}$$

where $H_{\mu\nu}(k)$ is defined by

$$H_{\mu\nu}(k) = \frac{1}{k^2 - M_\rho^2} (g_{\mu\nu} k^2 - k_\mu k_\nu). \tag{3.19}$$

It is an easy algebraic task to confirm that the identity (3.14) holds now. In order to consider the recovery of Ward identity in more detail, we may add the $k_\mu k_\nu / M_\rho^2$ -term to each ρ -meson propagator in Eq. (3.17) by treating it as massive vector meson

$$g_{\mu\nu} \frac{M_\rho^2}{M_\rho^2 - k^2} \rightarrow \frac{M_\rho^2}{M_\rho^2 - k^2} \left(g_{\mu\nu} - \frac{k_\mu k_\nu}{M_\rho^2} \right) = g_{\mu\nu} - H_{\mu\nu}(k). \tag{3.20}$$

Then the expression (3.17) becomes

$$\begin{aligned}
G_{\mu\nu}(q, k; p_1, p_2) &= -e \left[2 \left\{ g_{\mu\nu} - H_{\mu\nu}(k) - H_{\mu\nu}(q) + H_{\nu\beta}(k) H_{\mu}^\beta(q) \right\} \right. \\
&\quad \left. - \frac{1}{(k + p_2)^2 - m_\pi^2} \left\{ g_{\nu\beta} - H_{\nu\beta}(k) \right\} (2p_2 + k)^\beta \left\{ g_{\mu\alpha} - H_{\mu\alpha}(q) \right\} (2p_1 + q)^\alpha \right]
\end{aligned}$$

$$\Gamma_\mu(k; p_1, p_2) = e (g_{\mu\beta} - H_{\mu\beta}(k)) (p_1 + p_2)^\beta \left[-\frac{1}{(p_1 - k)^2 - m_\pi^2} \{g_{\nu\beta} - H_{\nu\beta}(k)\} (2p_1 - k)^\beta \{g_{\mu\alpha} - H_{\mu\alpha}(q)\} (2p_2 - q)^\alpha \right], \quad (3.21)$$

The comparison of Eqs. (3.21) and (3.18) with $a = 2$ shows that the absence of the $H_{\beta\nu}(k)H_{\mu}^\beta(q)$ term in (3.18) is responsible for the recovery of the identity (3.14). This is a consequence of the nonexistence of the direct $\rho^0\rho^0\pi^+\pi^-$ -term, as has been stressed in Sec. III A. This argument applies equally well to the light-by-light scattering amplitude caused by a charged pion loop.

C. Muon Anomaly

We can now evaluate contributions of diagrams of Fig. 2 to the muon anomaly a_μ . Let the vertex correction from a diagram S be denoted as $\Lambda_S^\nu(p, q)$ for the incoming photon momentum q , apart from the factor "ie". Then the contribution to a_μ from the diagram S is given by

$$a_\mu(S) = \lim_{p, q, q^2 \rightarrow 0} \text{Tr} (P_\nu(p, q) \Lambda_S^\nu(p, q)), \quad (3.22)$$

where $P_\nu(p, q)$ is the magnetic moment projection operator

$$P_\nu(p, q) = \frac{1}{16} \left(\not{p} - \frac{\not{q}}{2} + 1 \right) (\gamma_\nu \not{q} - \not{q} \gamma_\nu - 3p_\nu q \cdot q) \left(\not{p} + \frac{\not{q}}{2} + 1 \right), \quad (3.23)$$

with the muon mass m_μ set equal to 1. The diagrams constructed from the interactions in Eq. (3.8) can be classified in the similar manner as in Fig. 5 of Ref. [5]. However, let us recall that the replacement (2.1) performed in the VMD model of [5] works only if the $\rho^0\rho^0\pi^+\pi^-$ coupling term is present. In a theory with HLS (restricted for simplicity to the case of complete vector meson dominance ($a = 2$)), however, there is no such term. This means that, while the replacement of the photon propagator (3.15) by (3.16) is performed as before if the photon line is connected to the pion through the $\gamma\pi^+\pi^-$ coupling, the replacement must be carried out for either one of the lines but *not for both*, if the photon lines comes from a $\gamma\gamma\pi^+\pi^-$ coupling. As a consequence, the contribution $a_\mu(\text{HLS}; A_2)$ from the diagram in

Fig. 4 (which is topologically the same as the diagram A_2 in Fig. 5 of Ref. [5]), for instance, takes the form

$$a_\mu(\text{HLS}; A_2) = a_\mu(\text{sQED}; A_2) - a_\mu(\text{sQED}; (A_2, 2)) - a_\mu(\text{sQED}; (A_2, 3)) - a_\mu(\text{sQED}; (A_2, 4)) \\ + a_\mu(\text{sQED}; (A_2, \{2, 3\})) + a_\mu(\text{sQED}; (A_2, \{3, 4\})), \quad (3.24)$$

where $a_\mu(\text{sQED}; (A_2, \{2, 3, \dots\}))$ denotes the quantity obtained by replacing the photon propagators of the lines 2, 3, \dots with the propagators of mass M_ρ . This differs from the calculation of Ref. [5] by the absence of the terms

$$+ a_\mu(\text{sQED}; (A_2, \{2, 4\})) - a_\mu(\text{sQED}; (A_2, \{3, 2, 4\})). \quad (3.25)$$

Since the $\gamma\pi^+\pi^-$ vertex receives no modification, the contributions of the diagrams $C_1 - C_4$ in Ref. [5] remain unaltered.

The prescription for numerical evaluation of Feynman integrals follows that described in Ref. [26]. As in scalar QED, the B'_{ij} which appears on the right-hand-side of Eq. (37) of Ref. [26] must be changed to B_{ij} . The correctness of this change can be shown explicitly in the same manner as in the Appendix B of Ref. [5]. The renormalization [27] is required for calculating individual diagram since each diagram, not being gauge-invariant, has logarithmic divergence residing in the hadronic light-by-light scattering subdiagram. The evaluation of integrals is performed with the help of the Monte Carlo integration routine VEGAS [28].

Let us now summarize our results. To begin with we checked the scalar QED result in (2.2) by writing new FORTRAN programs from the scratch. The result (obtained using VEGAS with 40 million sampling points per iteration and 60 iterations) is

$$a_\mu(a, \text{sQED}) = -0.035\ 57\ (18) \left(\frac{\alpha}{\pi}\right)^3 \\ = -44.58\ (23) \times 10^{-11}, \quad (3.26)$$

confirming the previous result in (2.2) but, of course, with much higher precision. The new evaluation of the ρ -meson contribution in the HLS approach yields (for 40 million sampling points per iteration and 60 iterations)

$$\begin{aligned}
a_\mu(a, \text{HLS}) &= -0.003\ 55\ (12) \left(\frac{\alpha}{\pi}\right)^3 \\
&= -4.45\ (15) \times 10^{-11}.
\end{aligned}
\tag{3.27}$$

This result is about 3.5 times smaller than the VMD model result given in (2.3).

To see whether this reduction is real, we have evaluated the difference $a_\mu(a, \text{HLS}) - a_\mu(a, \text{nVMD})$ directly. The result is (for 40 million sampling points per iteration and 50 iterations)

$$\begin{aligned}
a_\mu(a, \text{HLS}) - a_\mu(a, \text{nVMD}) &= 0.009\ 76\ (4) \left(\frac{\alpha}{\pi}\right)^3 \\
&= 12.23\ (5) \times 10^{-11}.
\end{aligned}
\tag{3.28}$$

From (3.27) and (3.28) we obtain

$$\begin{aligned}
a_\mu(a, \text{nVMD}) &= -0.013\ 36\ (14) \left(\frac{\alpha}{\pi}\right)^3 \\
&= -16.74\ (18) \times 10^{-11},
\end{aligned}
\tag{3.29}$$

which is consistent with (2.3). Thus the numerical works check out and the difference (3.28) is real. Of course, the errors quoted above are those of numerical integration only and do not include estimates of model dependence.

D. Discussion of Large Momentum Contribution

As we have seen in the previous subsection, the ρ dominance structure has significant effects on the hadronic light-by-light scattering contribution to a_μ . In order to gain some insight in the dependence of $a_\mu(a; \text{HLS})$ on M_ρ and m_π , let us introduce a function $a_\mu(a; m, M)$, where $a_\mu(a; \text{HLS}) = a_\mu(a; m, M)$ for $m = m_\pi$ and $M = M_\rho$, and examine it as a function of m and M numerically. Table II contains the result for m_π (M_ρ) dependence obtained by 15 (30) iterations of Monte Carlo integration with one million sample points. From that table the following approximate asymptotic behaviors can be inferred:

$$a_\mu(a; xm_\pi, M) \sim -4.75 \times 10^{-2} \times x^{-2} \left(\frac{\alpha}{\pi}\right)^3 \quad \text{for } x \geq 3, M = \infty, \quad (3.30)$$

$$a_\mu(a; xm_\pi, M) \sim +2.81 \times 10^{-2} \times x^{-2} \left(\frac{\alpha}{\pi}\right)^3 \quad \text{for } x \geq 3, M = M_\rho, \quad (3.31)$$

$$a_\mu(a; m_\pi, M) \sim a_\mu(a; m_\pi, \infty) + 0.23 \left(\frac{m_\mu}{M}\right) \left(\frac{\alpha}{\pi}\right)^3 \quad \text{for } M > M_\rho, \quad (3.32)$$

where $a_\mu(a; m_\pi, \infty) = a_\mu(a, \text{sQED})$.

The results (3.30) and (3.31) show that $a_\mu(a; m, M)$ depends on the loop mass m asymptotically as m^{-2} for a wide range of “ ρ mass” M . To appreciate the significance of these results, note that, for $m \gg m_\pi$, m in $a_\mu(a; m_\pi, M) - a_\mu(a; m, M)$ may be regarded as a cut-off mass of the pion-loop momentum à la Pauli-Villars: The contribution of pion-loop momenta above m is suppressed in $a_\mu(a; m_\pi, M) - a_\mu(a; m, M)$. Thus the above dependences on m_π result from the fact that the contribution of pion loop momenta larger than m drops off as m^{-2} as m increases. For instance, the contribution of pion-loop momentum higher than 800 MeV occupies only 7 percent of the total contribution (3.26) or (3.27).

From these results, we speculate that the pion-loop light-by-light scattering amplitude (even with off shell photons) is governed by the region of small loop momenta carried by light hadrons.

The result (3.32) is inferred from the near constancy of $M(a_\mu(a; m_\pi, M) - a_\mu(a; m_\pi, \infty))$ for $M_\rho \leq M \leq 10M_\rho$. This function decreases very slowly for larger M . Such an M^{-1} (instead of M^{-2}) behavior seems to cast some doubt on the effectiveness of chiral perturbation theory since it implies that there is an appreciable contribution to $a_\mu(a, \text{HLS})$ from the region of photon momenta larger than M_ρ . To analyze this problem, let us recall that the customary argument in favor of the M^{-2} behavior is inferred from the fact that $-M_\rho^{-2}$ is the dominant term in the ρ -meson propagator:

$$\frac{1}{p^2 - M_\rho^2} = -\frac{1}{M_\rho^2} + \frac{p^2}{(p^2 - M_\rho^2)M_\rho^2} \quad (3.33)$$

for $|p^2| \ll M_\rho^2$. As is readily seen by power counting, however, naive evaluation of the contribution of each term on the right-hand side of Eq. (3.33) to $a_\mu(a, \text{HLS})$ leads to UV cut-off dependent results. In other words, the M^{-2} term has a divergent coefficient and

naive power counting argument fails. This is due to the fact that the $M_\rho \rightarrow \infty$ limit and sub-integrations in the Feynman diagram do not commute.

It is important to note, however, that the fact that photons of momenta larger than M_ρ contribute significantly to $a_\mu(a, \text{HLS})$ does not necessarily mean the failure of chiral perturbation theory. The requirement on the photon momentum, which is a vector sum of pion momenta, can be considerably less strict insofar as the contribution to $a_\mu(a, \text{HLS})$ comes mostly from small pion loop momenta. In fact this is what can be inferred from (3.30) and (3.31). For these reasons the M^{-1} behavior of (3.32) is not inconsistent with the chiral perturbation theory.

For $M = M_\rho$, (3.32) can be written as

$$a_\mu(a, \text{HLS}) \simeq \left(-0.035\ 57\ (18) + 0.23 \frac{m_\mu}{M_\rho} \right) \left(\frac{\alpha}{\pi} \right)^3, \quad (3.34)$$

where the first term is from (3.26). $a_\mu(a, \text{HLS})$ deviates from (3.34) for M_ρ smaller than the physical value. It is seen from (3.34) that the leading term happens to be nearly cancelled by the non-leading term for physical ρ mass. The smallness of the value (3.27) results from a (somewhat accidental) cancelation of $a_\mu(a, \text{sQED})$ and the $\mathcal{O}(m_\mu/M_\rho)$ term for the physical value of the ρ meson mass.

Before writing down our best estimate of the charged pion loop contribution to the muon $g - 2$, it must be recalled that the result (3.27) is based on the specific hadron model. In principle, any models which preserve chiral symmetry and the relevant Ward identities are the candidates for this computation. Any of these models is expected to lead to more or less the same hadronic light-by-light scattering amplitude provided that the chiral symmetry is intact. Eq. (3.34) indicates, however, that the large photon momenta give rise to significant contribution to a_μ . Thus the hadronic structure in photon beyond the ρ mass may be non-negligible. The model dependence may enter here.

In this computation, we have used the HLS approach. Even within this framework we assume further a complete ρ dominance. Also we could have chosen the version of HLS with higher resonances, such as A_1 . All these would increase the uncertainty of our result.

The previous work based on the ENJL model [13] asserts that the QED result of pion loop should be included from the standpoint of systematic chiral expansion. As was mentioned previously, the ENJL model Lagrangian is always written in the form consistent with HLS. Then the pion loop contribution in that model reduces to the one obtained here when we approximate more complicated form factor of $\pi^+\pi^-\gamma\gamma$ and $\pi^+\pi^-\gamma$ [29].

In spite of these model dependences, we expect the total error to be within 20 % of the difference $a_\mu(a, \text{HLS}) - a_\mu(a, \text{sQED})$. This is because integrations over the photon and muon momenta are convergent in these diagrams and hence the contribution of large photon momenta does not distort our picture of low energy pion loop too severely.

The kaon loop contribution is found to be about 4 % of the pion contribution. Taking these error estimates of the pion-loop and kaon-loop contributions into consideration, we present

$$\begin{aligned} a_\mu(a) &= -0.003\ 6\ (64) \left(\frac{\alpha}{\pi}\right)^3 \\ &= -4.5\ (8.1) \times 10^{-11}, \end{aligned} \tag{3.35}$$

as our best estimate, including model dependence, for the contribution to a_μ of the charged pion loop part of the hadronic light-by-light scattering amplitude. Eq. (3.35) replaces (2.3) obtained in Ref. [5] based on a naive vector meson dominance model which is inconsistent with the chiral symmetry.

IV. NEUTRAL PSEUDOSCALAR POLE

The first subsection here describes the detail of our prescription adopted in Ref. [12]. The second subsection describes extension of our method to include the pole-type axial contribution, and discusses the total contribution of this type.

A. Incorporation of Triangle Quark Loop

For the purpose of later comparison, we record again the result (2.5) for the neutral pion pole contribution $a_\mu(b)$ obtained in the HLS approach (for 5 million sampling points per iteration and 20 iterations):

$$\begin{aligned} a_\mu(b, \text{HLS}) &= -0.044\ 36\ (2) \left(\frac{\alpha}{\pi}\right)^3 \\ &= -55.60\ (3) \times 10^{-11}. \end{aligned} \quad (4.1)$$

Here we used the newly written FORTRAN programs for evaluating this result. Note that a sign error in some part of the integrand in [5] is corrected in (4.1).

It is far from certain that the off-shell behavior, in particular, with respect to the pion momentum, is well-approximated by the use of the effective interaction (2.4) modified by the HLS method. The examination of different off-shell extrapolation scheme will give some insight in the dependence of muon anomaly $a_\mu(b)$ on the off-shell behavior. Here we choose the diagram shown in Fig. 3, which is again suggested by the ENJL model, as a model for such an extrapolation scheme, and evaluate it explicitly.

Let us begin by noting that, in Fig. 3, the one-quark-loop subdiagram corresponding to $\pi^0(q) \rightarrow \gamma(p_1)\gamma(p_2)$ can be written as [30]

$$A_{\mu\nu}(p_1, p_2) = \epsilon_{\mu\nu\alpha\beta} p_1^\alpha p_2^\beta \frac{\alpha}{\pi f_\pi} \int [dz] \frac{2m_q^2}{m_q^2 - z_2 z_3 p_1^2 - z_3 z_1 p_2^2 - z_1 z_2 q^2}, \quad (4.2)$$

where $[dz] = dz_1 dz_2 dz_3 \delta(1 - (z_1 + z_2 + z_3))$. This amplitude is reduced to the one obtained from (2.4) in the limit $p_1^2 = p_2^2 = q^2 = 0$, showing that it is normalized correctly. Note that the insertion of (4.2) into the Feynman diagram of a_μ yields a convergent result without recourse to the VMD model. If we use the notation $a_\mu(b; m_\pi, M_\rho, m_q)$ in analogy with $a_\mu(a; m_\pi, M_\rho)$ in the case of $a_\mu(a)$, such a contribution corresponds to $a_\mu(b; m_\pi, \infty, m_q)$. The numerical evaluation can be carried out in a straightforward manner if we re-express (4.2) in the form of momentum integral representation and use the general formalism [26] for the evaluation of Feynman integral. The result is found to be (for 5 million sampling points per iteration and 20 iterations)

$$\begin{aligned}
a_\mu(b; m_\pi, \infty, m_q) &= -0.069\ 34\ (5) \left(\frac{\alpha}{\pi}\right)^3 \\
&= -86.90\ (7) \times 10^{-11},
\end{aligned}
\tag{4.3}$$

where we have chosen the quark mass to be 300 MeV. The operator product expansion analysis on the short distance behavior of the amplitude $A_{\alpha\beta}$ supports the use of constituent quark mass as m_q in Eq. (4.2) [31].

The diagram in Fig. 2(b), with the VMD assumption added, can be calculated in a similar manner. As has been noted in Sec. IIB, the coupling of quark to vector meson is obtained with the help of the ENJL model. As a result we obtain (for 5 million sampling points per iteration and 20 iterations)

$$\begin{aligned}
a_\mu(b) &= -0.026\ 94(5) \left(\frac{\alpha}{\pi}\right)^3 \\
&= -33.76\ (7) \times 10^{-11}.
\end{aligned}
\tag{4.4}$$

Here again, in order to examine what range of momentum governs $a_\mu(b)$, we perform the same analysis on $a_\mu(b; m_\pi, M_\rho, m_q)$, where m_q is constituent quark mass of the triangular loop, as has been done for $a_\mu(a; m_\pi, M_\rho)$. Table III lists the results for the quoted quantity for various values of m_π (or M_ρ) obtained by 20 (or 10) iterations of integration with 5 million sample points. For quark mass larger than 300 MeV, $a_\mu(b; m_\pi, M_\rho, m_q)$ approaches $a_\mu(b; \text{HLS})$ as m_q^{-2} , as is readily seen from the analytic expression for the triangle graph. For small m_q , it approaches zero. For instance, for $m_q = 5$ MeV, we have $a_\mu(b; m_\pi, M_\rho, m_q) = -0.666 \times 10^{-5}(\alpha/\pi)^3$. The results in Table III are summarized by the following asymptotic form:

$$a_\mu(b; xm_\pi, M_\rho, m_q) = -9.57 \times 10^{-2} \times x^{-2} \left(\frac{\alpha}{\pi}\right)^3 \quad \text{for } x \geq 3,
\tag{4.5}$$

$$a_\mu(b; m_\pi, M, m_q) = a_\mu(b; m_\pi, \infty, m_q) + 0.31 \left(\frac{m_\mu}{M}\right) \left(\frac{\alpha}{\pi}\right)^3 \quad \text{for } M \geq 3M_\rho.
\tag{4.6}$$

These results show that the same consideration as in Sec. IIID also applies here.

Note that the η pole contribution, when the mixing among π , η and η' is taken into account, amounts to 25 % of (4.4):

$$\begin{aligned}
a_\mu(\eta \text{ pole}) &= -0.005\,29\,(2) \times \left(\frac{\alpha}{\pi}\right)^3 \\
&= -7.305\,(3) \times 10^{-11},
\end{aligned}
\tag{4.7}$$

which is obtained using 5 million sampling points per iteration and 20 iterations. The ρ mass dependence of the η contribution is listed in Table IV (for 5 million sampling points per iteration and 10 iterations). From this Table we obtain an approximate asymptotic formula

$$a_\mu(b; m_\eta, M, m_q) = a_\mu(b; m_\eta, \infty, m_q) + 0.11 \left(\frac{m_\mu}{M}\right) \times \left(\frac{\alpha}{\pi}\right)^3 \quad \text{for } M \geq 3M_\rho, \tag{4.8}$$

where

$$\begin{aligned}
a_\mu(b; m_\eta, \infty, m_q) &= -0.020\,08\,(1) \times \left(\frac{\alpha}{\pi}\right)^3, \\
&= -25.17\,(2) \times 10^{-11}.
\end{aligned}
\tag{4.9}$$

This was obtained for 5 million sampling points per iteration and 20 iterations.

Adding (4.4) and (4.7) and again estimating the model dependence to be within about 20 % of the M_ρ -dependent term, we obtain

$$\begin{aligned}
a_\mu(b) &= -0.032\,2\,(66) \left(\frac{\alpha}{\pi}\right)^3 \\
&= -40.4\,(8.3) \times 10^{-11}.
\end{aligned}
\tag{4.10}$$

This is the result for the pseudoscalar pole contribution given in Ref. [12].

Further discussion of the off-mass-shell behavior of the $\pi^0\gamma^*\gamma^*$ vertex is given in Sec. VI.

B. Further Examination of the Pole Contribution

After our summarizing paper, Ref. [12], was submitted for publication, we learned that the hadronic light-by-light scattering contribution to the muon $g - 2$ has also been studied by another group [14] in the large N_C limit within the framework of the ENJL model. Their initial result for the contribution corresponding to Fig. 2(b) disagreed strongly with our

result. Since then, however, it was found that this was due to a simple numerical oversight [15]. Correction of this error brings their result closer to our $a_\mu(b)$. Nevertheless, their report [14] stimulated our interest to study the axialvector pole contribution in some detail.

In order to facilitate comparison with the results of [14], we follow their method closely. In particular we use the notation which enables us to keep track of the normalization factor directly. For the operator $j_5 \equiv \bar{q}T^3i\gamma_5q$, $j_\mu^Q \equiv \bar{q}Q\gamma_\mu q$, where the isospin generator T^3 is normalized as $2\text{tr}(T^3T^3) = 1$, the PVV (pseudoscalar-vector-vector) three-point function is defined as

$$\Pi_{\mu\nu}^{\text{PVV}}(p_1, p_2) \equiv i^2 \int d^4x_1 e^{ip_1 \cdot x_1} \int d^4x_2 e^{ip_2 \cdot x_2} \langle 0 | T j_5(0) j_\mu^Q(x_1) j_\nu^Q(x_2) | 0 \rangle. \quad (4.11)$$

The part of $\Pi_{\mu\nu}^{\text{PVV}}(p_1, p_2)$ corresponding to the 1-loop contribution, $\bar{\Pi}_{\mu\nu}^{\text{PVV}}(p_1, p_2)$, is given by the well-known triangle loop graph

$$\begin{aligned} \bar{\Pi}_{\mu\nu}^{\text{PVV}}(p_1, p_2) &= -\frac{2}{m_q} \frac{1}{16\pi^2} \epsilon_{\mu\nu\alpha\beta} p_1^\alpha p_2^\beta F(p_1^2, p_2^2, q^2), \\ F(p_1^2, p_2^2, q^2) &= 1 + I_3(p_1^2, p_2^2, q^2) - I_3(0, 0, 0), \\ I_3(p_1^2, p_2^2, q^2) &= 2m_q^2 \int dz_1 dz_2 dz_3 \delta(z_1 + z_2 + z_3 - 1) \frac{\Gamma(1, \tilde{M}^2(z_\alpha)/\Lambda_\chi^2)}{\tilde{M}^2(z_\alpha)}, \\ \tilde{M}^2(z_\alpha) &= m_q^2 - p_1^2 z_2 z_3 - p_2^2 z_3 z_1 - q^2 z_1 z_2, \end{aligned} \quad (4.12)$$

where Λ_χ is the momentum-cutoff which renders the quark loop contribution finite, m_q is the constituent quark mass, and $\Gamma(n, x)$ is the incomplete gamma function

$$\Gamma(n, x) = \int_x^\infty dt e^{-t} t^{n-1}. \quad (4.13)$$

The leading $1/N_C$ term of $\Pi_{\mu\nu}^{\text{PVV}}(p_1, p_2)$ can be written as [32]

$$\begin{aligned} \Pi_{\mu\nu}^{\text{PVV}}(p_1, p_2) &= -\frac{1}{16\pi^2} \epsilon_{\mu\nu\alpha\beta} p_1^\alpha p_2^\beta \frac{4m_q}{g_S f_\pi^2(-q^2) (m_\pi^2(-q^2) - q^2)} \\ &\quad \times \left[1 - g_A(-q^2) \left\{ 1 - F(p_1^2, p_2^2, q^2) L(p_1^2, p_2^2) \right\} \right], \end{aligned} \quad (4.14)$$

where

$$L(p_1^2, p_2^2) = \frac{M_V^2(-p_1^2) M_V^2(-p_2^2)}{\{M_V^2(-p_1^2) - p_1^2\} \{M_V^2(-p_2^2) - p_2^2\}}. \quad (4.15)$$

and $g_S = 8\pi^2 G_S / N_C \Lambda_\chi^2$ is the scalar coupling constant in the ENJL Lagrangian

$$\begin{aligned} \mathcal{L}_{\text{ENJL}}^{(\text{int.})} &= \frac{8\pi^2 G_S}{N_C \Lambda_\chi^2} \sum_{i,j} (\bar{q}_R^i q_{Lj}) (\bar{q}_L^j q_{Ri}) \\ &\quad - \frac{8\pi^2 G_V}{N_C \Lambda_\chi^2} \sum_{i,j} \left\{ (\bar{q}_L^i \gamma^\mu q_{Lj}) (\bar{q}_L^j \gamma_\mu q_{Li}) + (\bar{q}_R^i \gamma^\mu q_{Rj}) (\bar{q}_R^j \gamma_\mu q_{Ri}) \right\}. \end{aligned} \quad (4.16)$$

Here i and j represent the flavor indices, N_C is the number of colors and the parentheses assume the implicit sum over colors. The definition of various functions appearing in Eq.(4.14) can be found in Ref. [32].

Next we turn our attention to the AVV (axialvector-vector-vector) three-point function defined by

$$\Pi_{\alpha\mu\nu}^{\text{AVV}}(p_1, p_2) = i^2 \int d^4 x_1 e^{ip_1 \cdot x_1} \int d^4 x_2 e^{ip_2 \cdot x_2} \langle 0 | T j_{5\alpha}(0) j_\mu^Q(x_1) j_\nu^Q(x_2) | 0 \rangle. \quad (4.17)$$

where $j_{5\mu} \equiv \bar{q} \gamma_\mu \gamma_5 T^3 q$. A direct evaluation gives

$$\begin{aligned} \Pi_{\alpha\mu\nu}^{\text{AVV}}(p_1, p_2) &= L(p_1^2, p_2^2) \left[g_A(-q^2) \frac{M_A^2(-q^2)}{M_A^2(-q^2) - q^2} \bar{\Pi}_{\alpha\mu\nu}^{\text{AVV}}(p_1, p_2) \right. \\ &\quad \left. - 2m_q g_A(-q^2) \frac{1}{M_A^2(-q^2) - q^2} i q_\alpha \bar{\Pi}_{\mu\nu}^{\text{PVV}}(p_1, p_2) \right. \\ &\quad \left. + 2m_q g_A(-q^2) \frac{1}{m_\pi^2(-q^2) - q^2} i q_\alpha \bar{\Pi}_{\mu\nu}^{\text{PVV}}(p_1, p_2) \right] \\ &\quad + 2m_q g_A(-q^2) \frac{1}{M_A^2(-q^2) - q^2} i q_\alpha \bar{\Pi}_{\mu\nu}^{\text{PVV}}(p_1, p_2) \Big|_{p_1^2=0=p_2^2=q^2} \\ &\quad + 2m_q (1 - g_A(-q^2)) \frac{1}{m_\pi^2(-q^2) - q^2} i q_\alpha \bar{\Pi}_{\mu\nu}^{\text{PVV}}(p_1, p_2) \Big|_{p_1^2=0=p_2^2=q^2}, \end{aligned} \quad (4.18)$$

where $\bar{\Pi}_{\mu\nu}^{\text{PVV}}(p_1, p_2)$ is the 1-loop contribution of $\Pi_{\mu\nu}^{\text{PVV}}(p_1, p_2)$. $\bar{\Pi}_{\alpha\mu\nu}^{\text{AVV}}(p_1, p_2)$ is a linearly divergent integral

$$\bar{\Pi}_{\alpha\mu\nu}^{\text{AVV}}(p_1, p_2) = \frac{1}{2} i^2 \int \frac{d^4 r}{(2\pi)^4} (-1) \text{tr} \left[\gamma_\alpha \gamma_5 \frac{i}{\not{r} + \not{p}_1 - m_q} \gamma_\mu \frac{i}{\not{r} - m_q} \gamma_\nu \frac{i}{\not{r} - \not{p}_2 - m_q} \right], \quad (4.19)$$

where Pauli-Villars regularization is understood. The last two terms of (4.19) come from the presence of anomaly contribution when $-iq^\lambda \bar{\Pi}_{\lambda\mu\nu}^{\text{AVV}}(p_1, p_2)$ is rewritten in terms of $\bar{\Pi}_{\mu\nu}^{\text{PVV}}(p_1, p_2)$:

$$-iq^\lambda \bar{\Pi}_{\lambda\mu\nu}^{\text{AVV}}(p_1, p_2) L(p_1^2, p_2^2) = 2m_q \left\{ \bar{\Pi}_{\mu\nu}^{\text{PVV}}(p_1, p_2) L(p_1, p_2) - \bar{\Pi}_{\mu\nu}^{\text{PVV}}(p_1, p_2) \Big|_{p_1^2=p_2^2=q^2=0} \right\}, \quad (4.20)$$

a relation which was also used to derive Eq. (4.14).

Now the contributions of pseudoscalar and axial vector intermediate states to the four-photon vertex graph can be written, for instance, as

$$(ie)^4 \left[(2ig_S) \Pi_{\mu\nu}^{\text{P}VV}(p_1, p_2) \bar{\Pi}_{\rho\sigma}^{\text{P}VV}(p_3, p_4) L(p_3^2, p_4^2) + \left(-2i \frac{8\pi^2 G_V}{N_C \Lambda_\chi^2} \right) \Pi_{\alpha\mu\nu}^{\text{A}VV}(p_1, p_2) \bar{\Pi}^{\text{A}VV \alpha}_{\rho\sigma}(p_3, p_4) L(p_3^2, p_4^2) \right]. \quad (4.21)$$

The pseudoscalar pole contribution can be extracted from (4.21):

$$i\hat{A}_{\mu\nu}(p_1, p_2) \frac{i}{q^2 - m_\pi^2(-q^2)} i\hat{A}_{\rho\sigma}(p_3, p_4), \quad (4.22)$$

where

$$\begin{aligned} \hat{A}_{\mu\nu}(p_1, p_2) &\equiv -\frac{8\pi\alpha m_q}{2f_\pi(-q^2)} \bar{\Pi}_{\mu\nu}^{\text{P}VV}(p_1, p_2) \\ &= \frac{\alpha}{\pi f_\pi(-q^2)} \left[1 - g_A(-q^2) \left\{ 1 - F(p_1^2, p_2^2, q^2) L(p_1^2, p_2^2) \right\} \right]. \end{aligned} \quad (4.23)$$

For the following analysis, momentum dependences of various functions will be ignored: $f_\pi^2(-q^2) \simeq f_\pi^2$, $M_V^2(-q^2) \simeq M_\rho^2$, $g_A(-q^2) \simeq g_A$, $q^2 - m_\pi^2(-q^2) \simeq A^2(q^2 - m_\pi^2)$ with A accounting for the wave function renormalization constant of pion

$$A^2 = 1 - \left. \frac{\partial m_\pi^2(-p^2)}{\partial p^2} \right|_{p^2=m_\pi^2}, \quad (4.24)$$

which is close (and therefore set equal) to unity, and Λ_χ is taken as ∞ . In this approximation Eq. (4.22) reduces to

$$iA_{\mu\nu}(p_1, p_2) \frac{i}{q^2 - m_\pi^2} iA_{\rho\sigma}(p_3, p_4), \quad (4.25)$$

where the amplitude shown in (4.2), multiplied by a function $L(p_1^2, p_2^2)$ associated with vector meson dominance, is modified to

$$A_{\mu\nu}(p_1, p_2) = \frac{\alpha}{\pi f_\pi} \epsilon_{\mu\nu\beta\rho} p_1^\beta p_2^\rho F_{\text{P}VV}(p_1^2, p_2^2, q^2), \quad (4.26)$$

$$F_{\text{P}VV}(p_1^2, p_2^2, q^2) = \frac{1}{A} \left\{ 1 - g_A \left(1 - F(p_1^2, p_2^2, q^2) L(p_1^2, p_2^2) \right) \right\}. \quad (4.27)$$

The formal limit $g_A \rightarrow 1$ while keeping $M_V^2(-q^2)$ at a fixed finite value M_ρ^2 reduces (4.26) to (4.2) multiplied by $L(p_1^2, p_2^2)$. But such a limiting procedure is not self-consistent in the framework of the ENJL model. The term $(1-g_A)$ in (4.27) corresponds to the term necessary in order to recover the anomalous Ward identity missing in (4.2) as claimed in Ref. [14].

The contribution to the muon anomaly from the type of the graphs in Fig. 3 can be written as the magnetic moment projection (see Sec. III C) of

$$\begin{aligned} & \frac{2}{ie} \times \int \prod_{s=1}^2 \frac{d^4 r_s}{(2\pi)^4} (ie\gamma^\lambda) \frac{i}{\not{p}_6 - m_\mu} (ie\gamma^\beta) \frac{i}{\not{p}_5 - m_\mu} (ie\gamma^\alpha) \\ & \times \frac{-i}{p_1^2} \frac{-i}{p_2^2} \frac{-i}{p_3^2} \frac{i}{p_4^2 - m_\pi^2} iA_{\alpha\beta}(p_1, p_2) iA_{\lambda\nu}(p_3, q), \end{aligned} \quad (4.28)$$

which includes the symmetry factor 2 and an approximation $A^2 \simeq 1$. The internal lines are labeled according to Fig. 3. The terms of $F_{\text{PVV}}(p_1^2, p_2^2, q^2)$ in (4.27) consists of the point-like part, $(1-g_A)$, and the rest, $g_A F(p_1^2, p_2^2, q^2) L(p_1^2, p_2^2)$. Thus the term proportional to $(1-g_A)^2$ in the product of two $A_{\mu\nu}$'s in (4.28) corresponds to the contribution which includes two point-like vertices which causes logarithmic divergence from the photon loop integration. This is handled by introducing the Feynman cutoff for the photon propagators

$$\frac{-i}{q^2} \rightarrow \frac{-i}{q^2} - \frac{-i}{q^2 - M_c^2} = \frac{-iM_c^2}{q^2(M_c^2 - q^2)}. \quad (4.29)$$

This procedure is formally the same as that used for incorporating the vector meson dominance property in (4.1) but with a new mass scale M_c instead of M_ρ . This allows us to check the program written for the present purpose. When M_c is set equal to M_ρ , the result (4.1) should be identical with the result of $g_A = 0$, and the result (4.4) should correspond to that of $g_A = 1$. This is explicitly confirmed by our program. We have also confirmed that the results corresponding to various values of g_A ($0 \leq g_A \leq 1$) always falls in the range between (4.4) and (4.1) for $M_c = M_\rho$. In this way it is quite easy to observe that for any g_A and M_c , the cancelation among various terms cannot occur for the pseudoscalar pole contribution because all terms contribute with the same (negative) sign. Typical values of the π^0 -pole contribution obtained for various values of g_A and M_c are listed in Table V (10 million sampling points per iteration and 20 iterations for $g_A = 0.5$, 2 million sampling

points per iteration and 20 iterations for the other). Although our calculation is not exactly identical with that of Ref. [14] since we have disregarded the momentum dependence of $g_A(-q^2)$, etc., our result should be approximately equal to theirs. It turned out that we were not able to reproduce the result in Ref. [14].

The axial-vector meson contribution to four-photon vertex graph can also be extracted from (4.21)

$$\begin{aligned} & \left(i4\pi\alpha \frac{g_A}{f_A} \bar{\Pi}_{\alpha\mu\nu}^{\text{AVV}}(p_1, p_2) L(p_1^2, p_2^2) \right) \frac{-ig^{\alpha\beta}}{q^2 - M_A^2} \left(i4\pi\alpha \frac{g_A}{f_A} \bar{\Pi}_{\beta\rho\sigma}^{\text{AVV}}(p_3, p_4) L(p_3^2, p_4^2) \right) \\ & - \left(i4\pi\alpha \frac{g_A}{f_A} \frac{2m_q}{M_A} \left\{ \bar{\Pi}_{\mu\nu}^{\text{PVV}}(p_1, p_2) L(p_1^2, p_2^2) - \bar{\Pi}_{\mu\nu}^{\text{PVV}}(p_1, p_2) \Big|_{p_1^2=0=p_2^2=q^2} \right\} \right) \times \frac{-i}{q^2 - M_A^2} \\ & \times \left(i4\pi\alpha \frac{g_A}{f_A} \frac{2m_q}{M_A} \left\{ \bar{\Pi}_{\rho\sigma}^{\text{PVV}}(p_3, p_4) L(p_3^2, p_4^2) - \bar{\Pi}_{\rho\sigma}^{\text{PVV}}(p_3, p_4) \Big|_{p_3^2=0=p_4^2=q^2} \right\} \right). \end{aligned} \quad (4.30)$$

From Eq. (3.44) of Ref. [32], g_A/f_A is found to be independent of G_V . Thus, all contributions in Eq. (4.30) vanishes in the limit $M_A \rightarrow \infty$ ($G_V \rightarrow 0$), which, of course, should be the case. However the first term in Eq.(4.30) may become numerically significant since its overall coefficient

$$\left(\frac{g_A}{f_A} \right)^2 = g_A(1 - g_A) \left(\frac{M_A}{f_\pi} \right)^2, \quad (4.31)$$

where the equality is imposed by the ENJL model, is numerically large ~ 46 (for $g_A \sim 0.5$ [32]). Thus there remains a possibility that such a term contributes to the muon $g - 2$ with the same magnitude as pseudoscalar does, but with the opposite sign.

An explicit calculation shows that (for $g_A = 0.5$) the first term in (4.30), denoted as (1), and the second, denoted as (2), contribute respectively as

$$\begin{aligned} a_\mu(a_1 \text{ pole})[(1)] &= -0.001\,192\,(1) \times \left(\frac{\alpha}{\pi} \right)^3, \\ a_\mu(a_1 \text{ pole})[(2)] &= -0.000\,194\,(2) \times \left(\frac{\alpha}{\pi} \right)^3 \quad \text{for } M_c = 1.0 \text{ GeV}, \end{aligned} \quad (4.32)$$

The first one was calculated by 8 million sampling points per iteration and 15 iterations, the second by 3 million sampling points per iteration and 15 iterations.

We find that the axial-vector contribution has the same minus sign as the pseudoscalar one and is one order of magnitude smaller than the latter. Thus such a reduction of order

as was seen in Ref. [14] cannot take place according to our calculation. In this respect we are in agreement with the corrected result in Ref. [15].

The axial-vector pole contribution (4.32) is negligible as a pole-type contribution, compared to the pion pole. Adding the new evaluation of the η -pole contribution (5 million sampling points per iteration and 20 iterations)

$$\begin{aligned} a_\mu(\eta \text{ pole}) &= -0.011\ 69\ (1) \times \left(\frac{\alpha}{\pi}\right)^3 \\ &= -14.651\ (5) \times 10^{-11} \quad \text{for } g_A = 0.5, M_c = 1.0 \text{ GeV}, \end{aligned} \quad (4.33)$$

to the π^0 pole contribution given in Table V for $g_A = 0.5$ and $M_c = 1.0$ GeV, we obtain as the total pole contribution

$$\begin{aligned} a_\mu(b) &= -0.045\ 9\ (91) \times \left(\frac{\alpha}{\pi}\right)^3 \\ &= -57.5\ (11.4) \times 10^{-11}, \end{aligned} \quad (4.34)$$

where the model dependence is again estimated to be within 20 % of the M_ρ -dependent term. This replaces the value in (4.10) as the total pole contribution.

V. QUARK LOOP

Inferred from the ENJL model, the quark loop diagram incorporating vector meson can be calculated by making the substitution (2.1) to photon propagators. This leads to

$$\begin{aligned} a_\mu(c) &= 0.007\ 72\ (31) \left(\frac{\alpha}{\pi}\right)^3 \\ &= 9.68\ (39) \times 10^{-11}. \end{aligned} \quad (5.1)$$

To examine the quark mass dependence, we define $a_\mu(c; xm_q, M)$ with $a_\mu(c; m_q, M_\rho) \equiv a_\mu(c)$, where m_q denotes the collection of such masses as $m_u = m_d = 300\text{MeV}$ and $m_s = 500\text{MeV}$ and x the common scale factor. (Here we do not include c -quark contributions which have been included in the previous calculation [5] without VMD. Note that the c -quark contribution in this case is negligibly small since the contribution of each quark of mass m_q is

then proportional to m_q^{-2} [5]. The contribution of c -quark in the present model will be found as further suppressed as is inferred from the mass dependence presented below.) Numerical studies similar to the previous ones are performed to examine quark mass dependence by iterating integration with one billion sampling points per iteration and 60 iterations. The pion mass dependence is also examined by iterating integration with one million sampling points per iteration and 50 iterations.

The result is summarized in Table VI and in the following asymptotic form:

$$a_\mu(c; xm_q, M_\rho) \sim 1.94 \times 10^{-2} \times x^{-4.0} \left(\frac{\alpha}{\pi}\right)^3 \quad \text{for } x \geq 3, \quad (5.2)$$

$$a_\mu(c; m_q, M) \sim \left[+0.044 \ 0 - 0.43 \left(\frac{m_\mu}{M}\right)\right] \left(\frac{\alpha}{\pi}\right)^3 \quad \text{for } M \geq 3M_\rho. \quad (5.3)$$

Note that the suppression effect of vector meson is so large here that the value (5.1) is one order of magnitude smaller compared to (2.6). However the strong damping property on the quark mass is consistent with the observation that only the physical degree of freedom is important at low energies [33]. Algebraically such a rapid decrease occurs when all quark masses become comparable to M_ρ since the relevant mass scale of the system turns then to the quark masses so that the cancelation of the two terms in (2.1) begins.

Again, we consider the errors arising from model-dependence to be within 20 % of the M_ρ dependent term. This is because integrations over the photon and muon momenta are convergent in these diagrams and hence the contribution of large photon momenta does not distort our picture of low energy quark loop too severely. We are thus led to

$$\begin{aligned} a_\mu(c) &= 0.007 \ 7 \ (88) \left(\frac{\alpha}{\pi}\right)^3 \\ &= 9.7 \ (11.1) \times 10^{-11}. \end{aligned} \quad (5.4)$$

VI. SUMMARY AND DISCUSSION

We have obtained the results (3.35), (4.10) and (5.4) as the contributions of Fig. 2(a), (b) and (c), respectively. These diagrams have been discussed in Sec. II to contribute

most significantly and independently to the hadronic light-by-light scattering effect on muon anomaly a_μ , as guided by the use of chiral and $1/N_c$ expansion. The M_ρ dependence of the contributions (3.34), (4.6) and (5.3) indicates that the integration over the photon momenta receives considerable contribution from the region where photons are far off shell. We have estimated that these high mass contributions should be well within 20% of the vector meson contribution, which leads to the large uncertainties assigned to (3.35), (4.34) and (5.4). Combining these results we obtain

$$a_\mu(\text{light-by-light}) = -52 (18) \times 10^{-11}. \quad (6.1)$$

This is almost within the error (1.1) in the upcoming experiment. Therefore, with the progress of measurement of R [10], the accurate determination of muon anomaly by future experiment will actually show the presence of the weak interaction correction [4,34] and serves as a new constraint on physics beyond the standard model.

Let us now discuss possible causes of difference between our result and the recent result of Bijnens *et al.* [15], which is based on the ENJL model. For comparison's sake, let us list their results corresponding to Figs. 2(a), 2(b), and 2(c):

$$a_\mu(a)_{BPP} = (-14.5 \sim -22.8) \times 10^{-11} \quad (6.2)$$

for the cut-off μ ranging from 0.6 GeV to 4.0 GeV, and

$$a_\mu(b)_{BPP} = (-72 \sim -186) \times 10^{-11} \quad (6.3)$$

and

$$a_\mu(c)_{BPP} = (11.4 \sim 20.0) \times 10^{-11} \quad (6.4)$$

for the cut-off μ ranging from 0.7 GeV to 8.0 GeV.

On the surface, the results of [15] seems to be more reliable than ours, being less dependent on assumptions outside of the ENJL model. On the other hand, their result is not free from ambiguities either mainly because their theory does not tell which cut-off should be

avored. In particular, it seems to be difficult to justify their results for large μ which lies well beyond the region of applicability of the ENJL model.

The result (6.2) is about 4 times larger than our result (3.35). This may partly be due to our simplifying assumptions, such as the complete vector meson dominance ($a = 2$) and the neglect of momentum dependence of various masses and effective coupling constants. Note, however, that the Lagrangian of [15] seems to have the $\pi^+\pi^-\rho^0\rho^0$ vertex. The presence of such a coupling (without derivatives) will be inconsistent with the low energy phenomenology. It also means that their Lagrangian does not satisfy the Ward identity (3.14) contrary to their assertion. In particular, their Lagrangian does not seem to incorporate the vector meson consistently, as is described in detail in Appendix A. If this is the case, it could explain the bulk of the difference. It should also be recalled that the smallness of our result (3.35) is a consequence of an accidental cancelation of two main terms for the physical ρ mass value. Such a delicate cancelation is not visible in the calculation of [15].

The contribution (6.3) is 2 to 5 times larger than our estimate (4.10). Since this is the largest term, it is the main source of disagreement between the two calculations. Actually, the low end value (-72×10^{-11}) of (6.3) is of the same order of magnitude as our value for $a_\mu(b; m_\pi, \infty, m_q)$ given in (4.3). Recall that in the latter calculation the anomalous $\pi^0\gamma^*\gamma^*$ vertex is approximated by a triangular loop of constituent quarks and photons are attached to the “bare” quark directly. If one assumes that any QCD modification softens this coupling, our result (4.3) may be regarded as some sort of upper limit of the contribution of Fig. 2(b). On the other hand, the result (6.3) increases with increasing cut-off μ beyond this “bound”, suggesting that the result (6.3) diverges logarithmically as $\mu \rightarrow \infty$. This behavior is a consequence of the presence of a hard PVV vertex in their Lagrangian. Its prediction on the muon $g - 2$ must be viewed with severe reservation, however, since it is obtained by applying the ENJL model beyond its domain of validity determined by the cut-off Λ_χ . In fact, such an unwarranted application of the model (with a hard anomaly term) violates unitarity as γ^* goes far off shell [35], and hence must be tempered with some form factor. In other words, any realistic theory must be consistent with unitarity, be it the ENJL model

or the HLS model.

An examination of Fig. 3, in the limit where both fermion triangles shrink to points, shows that the UV divergence arises from the integration domain in which the momenta carried by the photon 3 and pion 4 are small while the momenta carried by the photons 1 and 2 are large. The far-off-shell structure of the $\pi^0\gamma^*\gamma^*$ vertex in such a region has been studied using the Bjorken-Johnson-Low theorem [36], which shows $1/q^2$ behavior asymptotically, where $q \sim q_1 \sim q_2$ [37]. The case where only one of the photons (q_2) is far off-shell has also been studied by an operator product expansion technique [38]. Based on the latter analysis a formula of the form interpolating between $p_1^2 = 0$ and $p_1^2 = \infty$

$$F(p_1^2 \rightarrow \infty, p_2^2 = 0, q^2) = \frac{1}{1 - (p_1^2/(8\pi^2 f_\pi^2))},$$

$$\sim \frac{1}{1 - (p_1^2/M^2)}, \quad (6.5)$$

has been suggested for the form factor $F(p_1^2, p_2^2, q^2)$ normalized similarly as that of (4.12). The experimental data fit Eq. (6.5) very well with $M^2 \sim (0.77 \text{ GeV}/c)^2$ over the range $2.0(\text{GeV}/c)^2$ to $20.0(\text{GeV}/c)^2$ [39]. In Ref. [21] it is argued that the off-shell behavior of the $\pi^0\gamma^*\gamma^*$ amplitude is represented reasonably well by the quark triangle amplitude (4.2) if one takes account of the asymptotic freedom of QCD and a nonperturbative generation of constituent quark mass. The result of their analysis is consistent with those quoted above. These considerations suggest that our model based on Eq. (4.2) may in fact be a reasonably good representation of the contribution of Fig. 2(b) [40].

There is relatively small difference between (6.4) and (5.4). The remaining difference is within the range of uncertainty caused by our simplifying assumptions. In fact the good agreement between (5.4) and (6.4) may even be an indication that we have overestimated the model dependence in (5.4). As was mentioned already, this is consistent with the fact that integrations over the photon and muon momenta are convergent and do not distort low energy quark-loop picture too severely.

It appears to be difficult to resolve the difference between our calculation and that of Ref. [15] completely because of different approaches and because of the necessity to apply the low

energy effective theory of strong interaction beyond its safely tested domain. The complete resolution may have to wait for the lattice QCD calculation of the four-point function. With the rapid improvement of the computing power, such a day may not be too far off.

ACKNOWLEDGMENTS

We acknowledge useful discussions with Bijnens, Pallante, and Prades. T. K. thanks S. Tanabashi and H. Kawai for helpful discussions. T. K.'s work is supported in part by the U. S. National Science Foundation. Part of numerical computation was carried out at the Cornell National Supercomputing Facility, which receives major funding from the U. S. National Science Foundation and the IBM Corporation, with additional support from New York State and members of the Corporate Research Institute. M. H. is supported in part by Japan Society for the Promotion of Science for Japanese Junior Scientists. He thanks the Toyota Physical and Chemical Research Institute for the support he has received in the early stage of this work. A. I. S. acknowledges a partial support from Daiko Foundation.

APPENDIX A: VECTOR MESON IN THE BPP CHIRAL LAGRANGIAN

In this Appendix we show that the vector meson is not properly incorporated as a dynamical field in the chiral Lagrangian (5.6) of Ref. [15]

$$\begin{aligned} \mathcal{L} = & \frac{f_\pi^2}{4} \text{tr} \left[\mathcal{D}_\mu U \mathcal{D}^\mu U^\dagger + \mathcal{M} U^\dagger + U \mathcal{M}^\dagger \right] \\ & + \frac{M_V^2}{2} \left[\left(\rho_\mu - \frac{1}{g} v_\mu \right) \left(\rho^\mu - \frac{1}{g} v^\mu \right) \right] + \frac{1}{8g^2} \text{tr} [L_{\mu\nu} L^{\mu\nu} + R_{\mu\nu} R^{\mu\nu}]. \end{aligned} \quad (\text{A1})$$

Here ρ_μ denotes vector meson field and \mathcal{M} represents the quark mass matrix, $\mathcal{M} = \text{diag}(m_u, m_d, m_s)$, in the three-flavor case. v_μ and a_μ are the external vector and axial-vector fields respectively, and $L_{\mu\nu}$ and $R_{\mu\nu}$ are given by

$$\begin{aligned} L_{\mu\nu} &= \partial_\mu (g\rho_\nu - a_\nu) - \partial_\nu (g\rho_\mu - a_\mu) + [(g\rho_\mu - a_\mu), (g\rho_\nu - a_\nu)] \\ R_{\mu\nu} &= \partial_\mu (g\rho_\nu + a_\nu) - \partial_\nu (g\rho_\mu + a_\mu) + [(g\rho_\mu + a_\mu), (g\rho_\nu + a_\nu)]. \end{aligned} \quad (\text{A2})$$

The transformation properties of v_μ , a_μ , ρ_μ , and the unitary matrix (U) consisting of the pseudoscalar meson are given by

$$U \rightarrow U' = V_R U V_L^\dagger, \quad (\text{A3})$$

$$(v_\mu + a_\mu) \rightarrow (v'_\mu + a'_\mu) = V_R(v_\mu + a_\mu)V_R^\dagger + iV_R\partial_\mu V_R^\dagger, \quad (\text{A4})$$

$$(v_\mu - a_\mu) \rightarrow (v'_\mu - a'_\mu) = V_L(v_\mu - a_\mu)V_L^\dagger + iV_L\partial_\mu V_L^\dagger, \quad (\text{A5})$$

$$(g\rho_\mu + a_\mu) \rightarrow (g\rho'_\mu + a'_\mu) = V_R(g\rho_\mu + a_\mu)V_R^\dagger + iV_R\partial_\mu V_R^\dagger, \quad (\text{A6})$$

$$(g\rho_\mu - a_\mu) \rightarrow (g\rho'_\mu - a'_\mu) = V_L(g\rho_\mu - a_\mu)V_L^\dagger + iV_L\partial_\mu V_L^\dagger \quad (\text{A7})$$

for the chiral transformation (V_L, V_R). Then the covariant derivative $\mathcal{D}_\mu U$:

$$\mathcal{D}_\mu U \equiv \partial_\mu U - i(g\rho_\mu + a_\mu)U + iU(g\rho_\mu - a_\mu), \quad (\text{A8})$$

in which vector meson ρ_μ appears instead of v_μ to realize the vector meson dominance, transforms covariantly. The vector meson mass term in (A1) is also chiral-invariant as shown below. (As a matter of fact it vanishes.)

The transformation property of the combination ($g\rho_\mu - v_\mu$) is found to be

$$\begin{aligned} (g\rho'_\mu - v'_\mu) &= (g\rho'_\mu + a'_\mu) - (v'_\mu + a'_\mu) \\ &= V_R(g\rho_\mu - a_\mu)V_R^\dagger \end{aligned} \quad (\text{A9})$$

from (A4) and (A6). On the other hand, from (A5) and (A7), we find

$$\begin{aligned} (g\rho'_\mu - v'_\mu) &= (g\rho'_\mu - a'_\mu) - (v'_\mu - a'_\mu) \\ &= V_L(g\rho_\mu - a_\mu)V_L^\dagger. \end{aligned} \quad (\text{A10})$$

Since V_L and V_R are independent, we may consider the case where $V_L = 1$ and V_R is nontrivial. Then, from Eqs. (A9) and (A10) we obtain

$$(g\rho_\mu - v_\mu) = V_R(g\rho_\mu - v_\mu)V_R^\dagger. \quad (\text{A11})$$

For simplicity, let us consider the two-flavor case, and set $V_R = e^{i\frac{\pi}{2}\sigma^2}$ (isospin rotation about the second axis). Then the RHS of eq. (A11) becomes

$$-(g\rho_\mu - v_\mu)^a \frac{\sigma^{a*}}{2}, \quad (\text{A12})$$

where “ $*$ ” denotes complex conjugation.

Picking up the third component of both sides of (A11), for instance, we get

$$(g\rho_\mu - v_\mu)^3 = -(g\rho_\mu - v_\mu)^3, \quad (\text{A13})$$

that is, $(g\rho_\mu - v_\mu)^3 = 0$.

In a similar way we can prove that $g\rho_\mu - v_\mu$ vanishes for other components. This means that ρ_μ is nothing but an external vector field and the vector meson has not been incorporated in the theory as a dynamical object.

REFERENCES

- [1] V. W. Hughes, in *Frontiers of High Energy Spin Physics* , edited by T. Hasegawa *et al.* (Universal Academy Press, Tokyo, 1992), pp. 717 - 722.
- [2] J. Bailey *et al.*, Phys. Lett. **68B**, 191 (1977); F. J. M. Farley and E. Picasso, in *Quantum Electrodynamics*, edited by T. Kinoshita (World Scientific, Singapore, 1990), pp. 479 - 559.
- [3] T. Kinoshita, in *Frontiers of High Energy Spin Physics* , edited by T. Hasegawa *et al.* (Universal Academy Press, Tokyo, 1992), pp. 9 - 18.
- [4] K. Fujikawa, B. W. Lee, and A. I. Sanda, Phys. Rev. D **6**, 2923 (1972); R. Jackiw and S. Weinberg, Phys. Rev. D **5**, 2473 (1972); G. Altarelli, N. Cabbibo, and L. Maiani, Phys. Lett. **40B**, 415 (1972); I. Bars and M. Yoshimura, Phys. Rev. D **6**, 374 (1972); W. A. Bardeen, R. Gastmans, and B. E. Lautrup, Nucl. Phys. **B46**, 319 (1972).
- [5] T. Kinoshita, B. Nižić, and Y. Okamoto, Phys. Rev D **31**, 2108 (1985).
- [6] C. Bouchiat and L. Michel, J. Phys. Radium **22**, 121 (1961); L. Durand, Phys. Rev. **128**, 441 (1962).
- [7] For recent attempts to evaluate $a_\mu(\text{had.v.p.})$ theoretically, see for example, E. Pallante, Phys. Lett. **B341**, 221 (1994), and Ref. [13].
- [8] J. A. Casas, C. López and F. J. Ynduráin, Phys. Rev. D **32**, 736 (1985); L. Martinovič and S. Dubnička, Phys. Rev. D **42**, 884 (1990); L. M. Kurdadze *et al.*, JETP Lett. **43**, 643 (1986); JETP Lett. **47**, 512 (1988); L. M. Barkov *et al.*, Sov. J. Nucl. Phys. **47**, 248 (1988); S. I. Dolinsky *et al.*, Phys. Rep. **C202**, 99 (1991); Phys. Lett. **B174**, 453 (1986);
- [9] S. Eidelman and F. Jegerlehner, Z. Phys. **C67**, 585 (1995).
- [10] W. A. Worstell and D. H. Brown, private communication.

- [11] P. Franzini, in “*Second DAΦNE Physics Handbook*”, edited by L. Maiani, L. Pancheri and N. Paver (INFN, Franzini, 1995) .
- [12] M. Hayakawa, T. Kinoshita and A. I. Sanda, Phys. Rev. Lett. **75**, 790 (1995).
- [13] E. de Rafael, Phys. Lett. **B322**, 239 (1994).
- [14] J. Bijnens, E. Pallante and J. Prades, Phys. Rev. Lett. **75**, 1447 (1995).
- [15] J. Bijnens, E. Pallante and J. Prades, Report No. NORDITA-95-75-N-P, 1995 (unpublished).
- [16] G. Ecker, J. Gasser, A. Pich and E. de Rafael, Nucl. Phys. **B321**, 311 (1989).
- [17] See Eqs. (3.10) and (3.24) of Ref. [5].
- [18] M. B. Einhorn, Phys. Rev. D **49**, 1668 (1993).
- [19] M. Bando, T. Kugo, and K. Yamawaki, Phys. Rep. **164** 217 (1988).
- [20] D. Atkinson, M. Harada and A. I. Sanda, Phys. Rev. D **46**, 3884 (1992).
- [21] M. Bando and M. Harada, Prog. Theor. Phys. **92**, 583 (1994).
- [22] D. Ebert and H. Reinhardt, Nucl. Phys. **B271**, 188 (1986).
- [23] J. Gasser and H. Leutwyler, Phys. Rep. **87**, 77 (1982).
- [24] Ö. Kaymakcalan and J. Schechter, Phys. Rev. D **31**, 1109 (1985).
- [25] Feynman gauge is chosen for the electromagnetic gauge fixing. In the calculation of the muon anomaly, the $k_\mu k_\nu$ part of the photon propagator is irrelevant due to the Ward identity. Likewise the $k_\mu k_\nu$ part of the ρ meson propagator drops out automatically in that case.
- [26] P. Cvitanović and T. Kinoshita, Phys. Rev. D **10**, 3978 (1974).
- [27] P. Cvitanović and T. Kinoshita, Phys. Rev. D **10**, 3991 (1974).

- [28] G. P. Lepage, J. Comput. Phys. **27**, 192 (1978).
- [29] We also expect, as in the ENJL model, that a q^2 -dependent function $M_V^2(q^2)$, where q is the ρ momentum, appears in place of the constant ρ meson mass. As is seen from the explicit form of $M_V^2(q^2)$ given in [13], the q^2 -dependence in the relevant range ($\leq M_\rho$) is relatively mild so that the correction to this approximation seems to be small.
- [30] See, for example, R. Jackiw, in *Current Algebra and Anomalies* (World Scientific, Singapore, 1985), pp. 81 - 210.
- [31] G. P. Lepage and S. J. Brodsky, Phys. Lett. **B87**, 359 (1979); A. Manohar, Phys. Lett. **B244**, 101 (1990).
- [32] J. Bijnens and J. Prades, Z. Phys. C **64**, 475 (1994).
- [33] One of the authors (A. I. S.) thanks S. Brodsky for discussion on this point.
- [34] T. V. Kukhto, E. A. Kuraev, A. Schiller, and Z. K. Silagadze, Nucl. Phys. B **371**, 567 (1992); A. Czarnecki, B. Krause, and W. J. Marciano, Phys. Rev. D **52**, 2619 (1995); S. Peris, M. Perrottet, and E. de Rafael, Phys. Lett. B **355**, 523 (1995).
- [35] K. Hikasa, Modern Phys. Lett. A **5**, 1801 (1990).
- [36] J.-M. Gérard and T. Lahna, Phys. Lett. B **356**, 381 (1995).
- [37] One of the authors (T. K.) thanks W. Marciano for calling his attention to Ref. [36].
- [38] S. J. Brodsky and G.P. Lepage, Phys. Rev. D **24**, 1808 (1981).
- [39] V. Savinov *et al.*, CLEO Collaboration, to be published in the proceedings of the international conference PHOTON'95 (Sheffield University, Sheffield, UK, April 1995).
- [40] The asymptotic behaviors given in [36] and [38] differ by some constant factor indicating the presence of some unresolved problem. However, both show q^{-2} -type damping for large q^2 , and that is the crucial point as far as our discussion is concerned.

TABLES

TABLE I. Orders with respect to $1/N_c$ and chiral expansions of the diagrams shown in Fig. 2.

Diagram	$1/N_c$ expansion	Chiral expansion
Fig. 2(a)	1	p^4
Fig. 2(b)	N_c	p^6
Fig. 2(c)	N_c	p^8

TABLE II. m_π and M_ρ dependence of π^\pm loop contribution. Table lists $(xm_\pi/m_\mu)^2 \times a_\mu(a; xm_\pi, M)$ for $M = M_\rho$ and $M = \infty$, and $(xM_\rho/m_\mu) \times [a_\mu(a; m_\pi, xM_\rho) - a_\mu(a; m_\pi, \infty)]$.

x	$(\pi/\alpha)^3 \times (xm_\pi/m_\mu)^2 \times a_\mu(a; xm_\pi, M_\rho)$	$(\pi/\alpha)^3 \times (xm_\pi/m_\mu)^2 \times a_\mu(a; xm_\pi, \infty)$	$(\pi/\alpha)^3 \times (xM_\rho/m_\mu) \times [a_\mu(a; m_\pi, xM_\rho) - a_\mu(a; m_\pi, \infty)]$
5	0.064 9 (44)	-0.082 (8)	0.234 (7)
10	0.094 5 (45)	-0.093 (9)	0.190 (7)
15	0.105 (4)	-0.099 (14)	0.155 (6)
20	0.106 (5)	-0.094 (17)	0.141 (6)
25	0.107 (5)	-0.094 (18)	0.124 (6)
30	0.110 (5)	-0.094 (25)	0.120 (6)

TABLE III. m_π and M_ρ dependence of π^0 pole contribution. Table lists $(xm_\pi/m_\mu)^2 \times a_\mu(b; xm_\pi, M_\rho, m_q)$ and $(xM_\rho/m_\mu) \times [a_\mu(b; m_\pi, xM_\rho, m_q) - a_\mu(b; m_\pi, \infty, m_q)]$.

x	$(\pi/\alpha)^3 \cdot (xm_\pi/m_\mu)^2 \times a_\mu(b; xm_\pi, M_\rho, m_q)$	$(\pi/\alpha)^3 \cdot (xM_\rho/m_\mu) \times [a_\mu(b; m_\pi, xM_\rho, m_q) - a_\mu(b; m_\pi, \infty, m_q)]$
5	-0.168 4 (1)	0.336 7 (2)
10	-0.203 4 (1)	0.276 5 (2)
15	-0.213 8 (1)	0.235 9 (2)
20	-0.218 2 (2)	0.207 3 (2)
25	-0.220 2 (2)	0.186 7 (2)
30	-0.221 5 (2)	0.170 1 (2)

TABLE IV. M_ρ dependence of η pole contribution. Table lists $(xM_\rho/m_\mu) \times [a_\mu(b; m_\pi, xM_\rho, m_q) - a_\mu(b; m_\pi, \infty, m_q)]$.

x	$(\pi/\alpha)^3 \cdot (xM_\rho/m_\mu) \times [a_\mu(b; m_\pi, xM_\rho, m_q) - a_\mu(b; m_\pi, \infty, m_q)]$
5	0.135 7 (8)
10	0.114 5 (8)
15	0.108 6 (7)
20	0.087 3 (5)
25	0.078 9 (5)
30	0.072 0 (5)

TABLE V. π^0 -pole contribution for various values of g_A and M_c . All the values are listed with the factor $(\alpha/\pi)^3$ removed.

g_A	$M_c = 1 \text{ GeV}$	$M_c = 2 \text{ GeV}$	$M_c = 4 \text{ GeV}$
0.3	- 0.053 85 (2)	- 0.089 58 (3)	- 0.137 35 (4)
0.5	- 0.034 18 (1)	- 0.057 06 (2)	- 0.086 20 (2)
0.8	- 0.036 43 (3)	- 0.044 03 (3)	- 0.052 67 (3)

TABLE VI. Quark mass and M_ρ dependence of quark loop contribution. Table lists $x^4 \times a_\mu(c; xm_q, M_\rho)$ and $(xM_\rho/m_\mu) \times [a_\mu(c; m_q, xM_\rho) - a_\mu(c; m_q, \infty)]$.

x	$(\pi/\alpha)^3 \times x^4 a_\mu(c; xm_q, M_\rho)$ $\times 10$	$(\pi/\alpha)^3 \times (xM_\rho/m_\mu)$ $\times [a_\mu(c; m_q, xM_\rho) - a_\mu(c; m_q, \infty)]$
5	0.177 (6)	- 0.489 (5)
10	0.198 (23)	- 0.486 (5)
15	0.191 (51)	- 0.460 (5)
20	0.193 (91)	- 0.423 (4)
25	0.195 (142)	- 0.402 (4)
30	0.194 (205)	- 0.385 (4)

FIGURES

FIG. 1. Hadronic light-by-light scattering (shown by the shaded blob) contribution to the muon anomaly. Solid line and dashed line represent muon and photon, respectively.

FIG. 2. Representative diagrams which dominate the hadronic light-by-light effect on a_μ at low energies. Other diagrams are obtained by permutation of the photon legs. (a) Charged pseudoscalar diagram in which the dotted line corresponds to π^\pm , etc. (b) One of the π^0 pole graphs, in which the dotted line corresponds to π^0 and the blob represents the $\pi\gamma\gamma$ vertex. (c) Quark loop contribution, where quark is denoted by bold line.

FIG. 3. Diagram of neutral pseudoscalar pole contribution with VMD and quark triangular loop. The bold dashed line represents the vector meson. The arrow attached to each internal line label indicates the direction of the corresponding momentum. Other diagrams are obtained by permutation of the photon legs.

FIG. 4. A typical diagram contributing to $a_\mu(a)$. To facilitate correspondence with the text, a number is attached to each internal line. Other diagrams are obtained by permutation of the photon legs.

M. H. [There is no meaning in the above letters. It is inserted for printing out all pages in the two-sides. (The total number of the files have to be odd, then. Sorry.)]

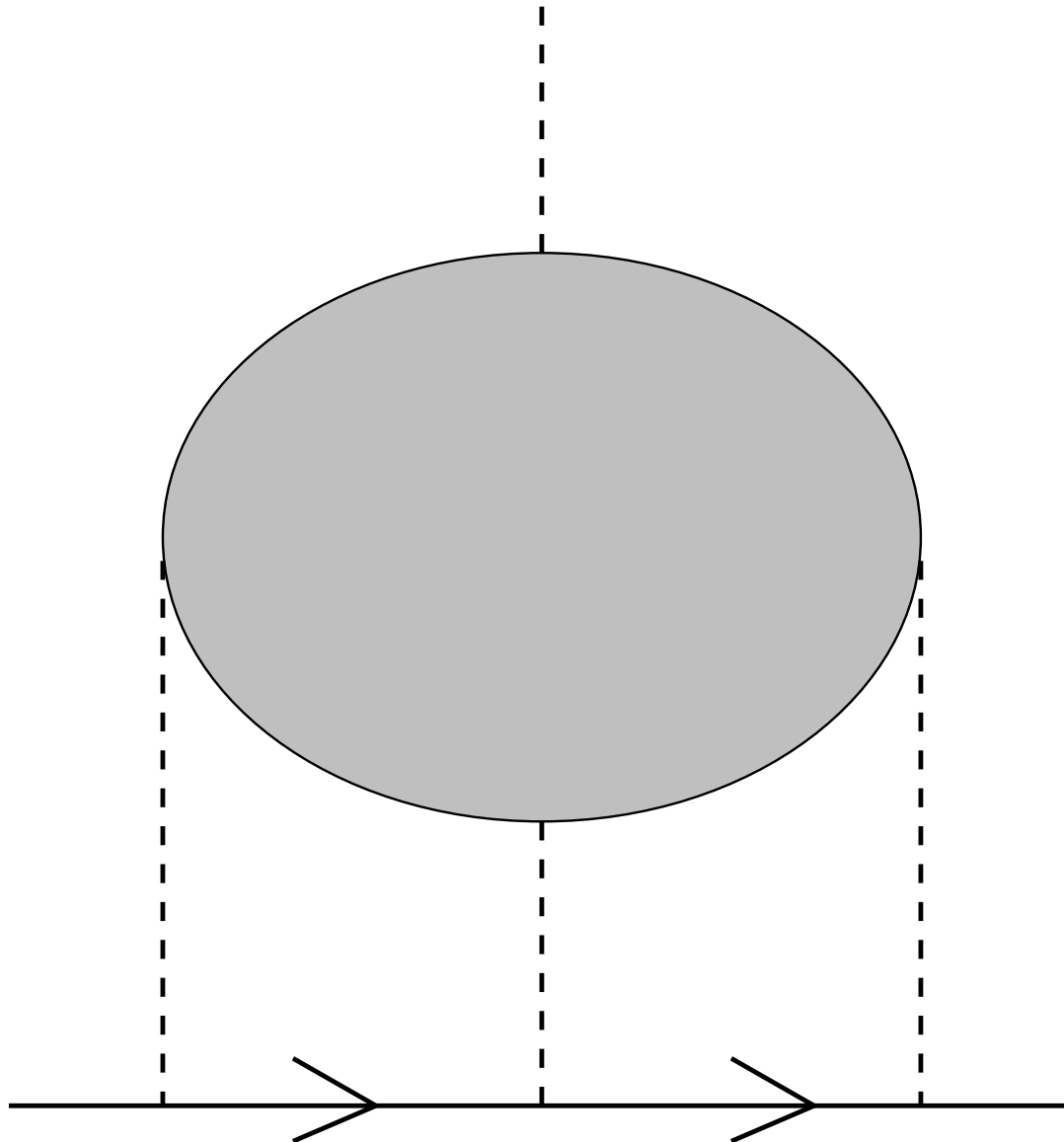


FIG. 1

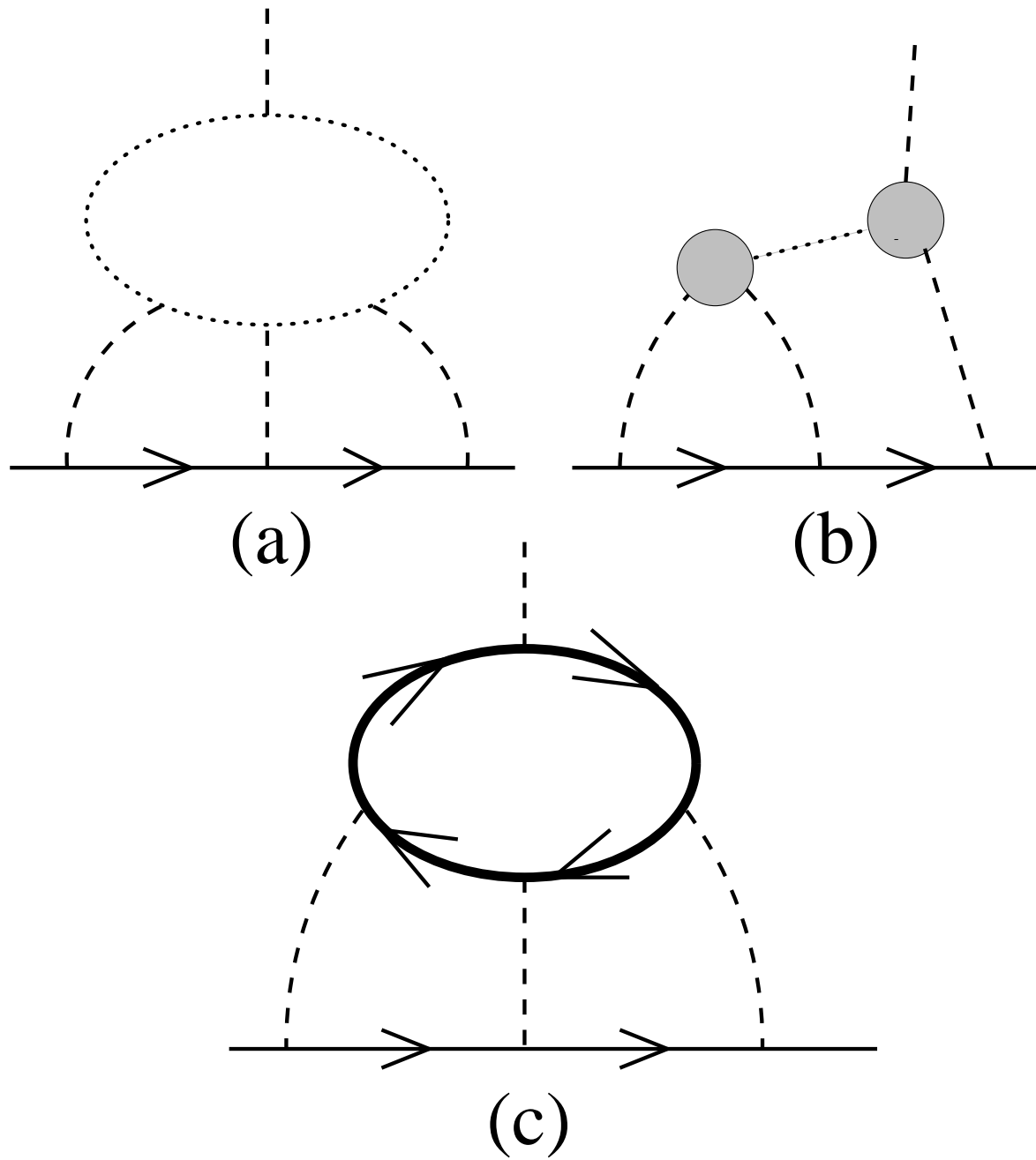


FIG. 2

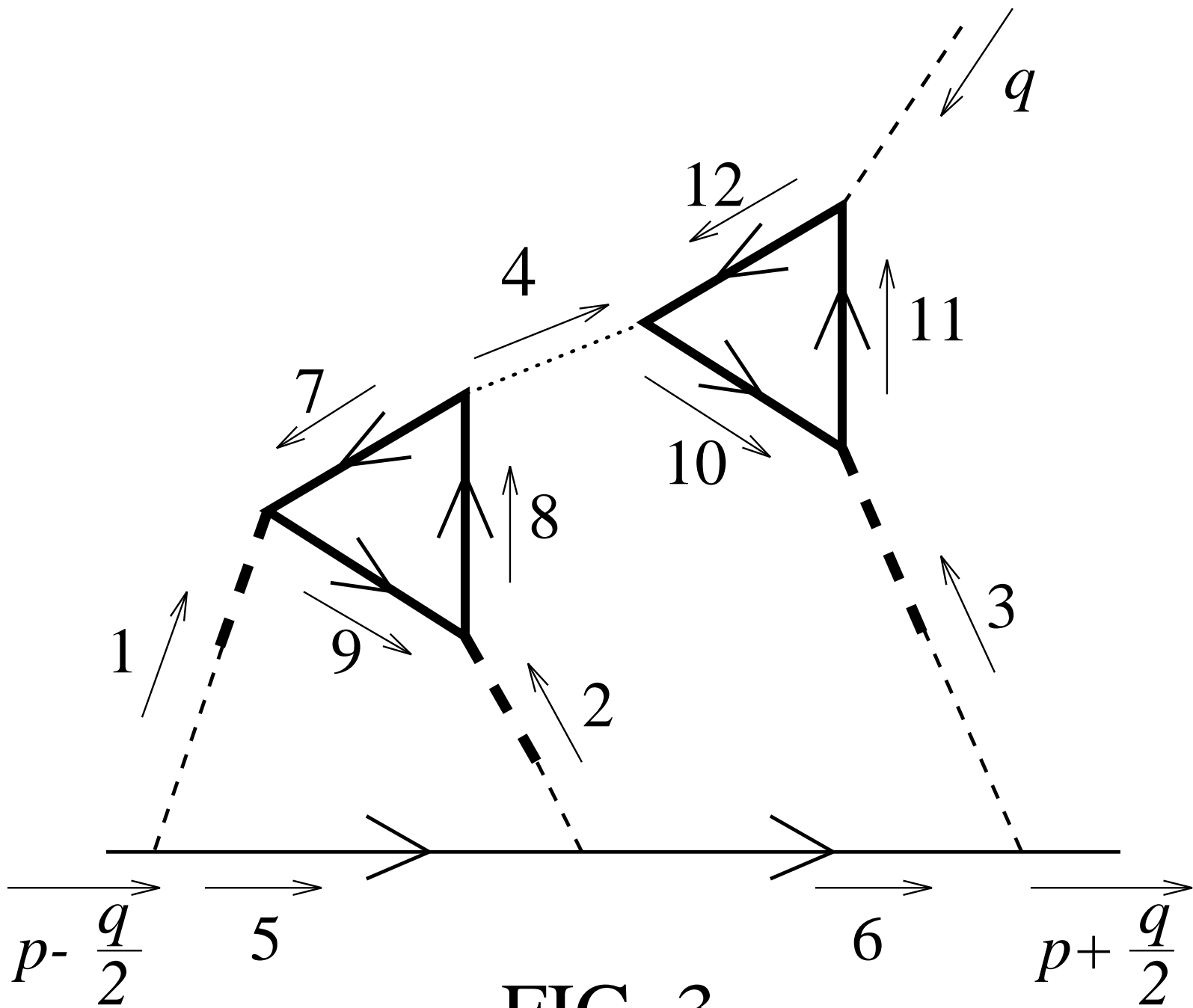


FIG. 3

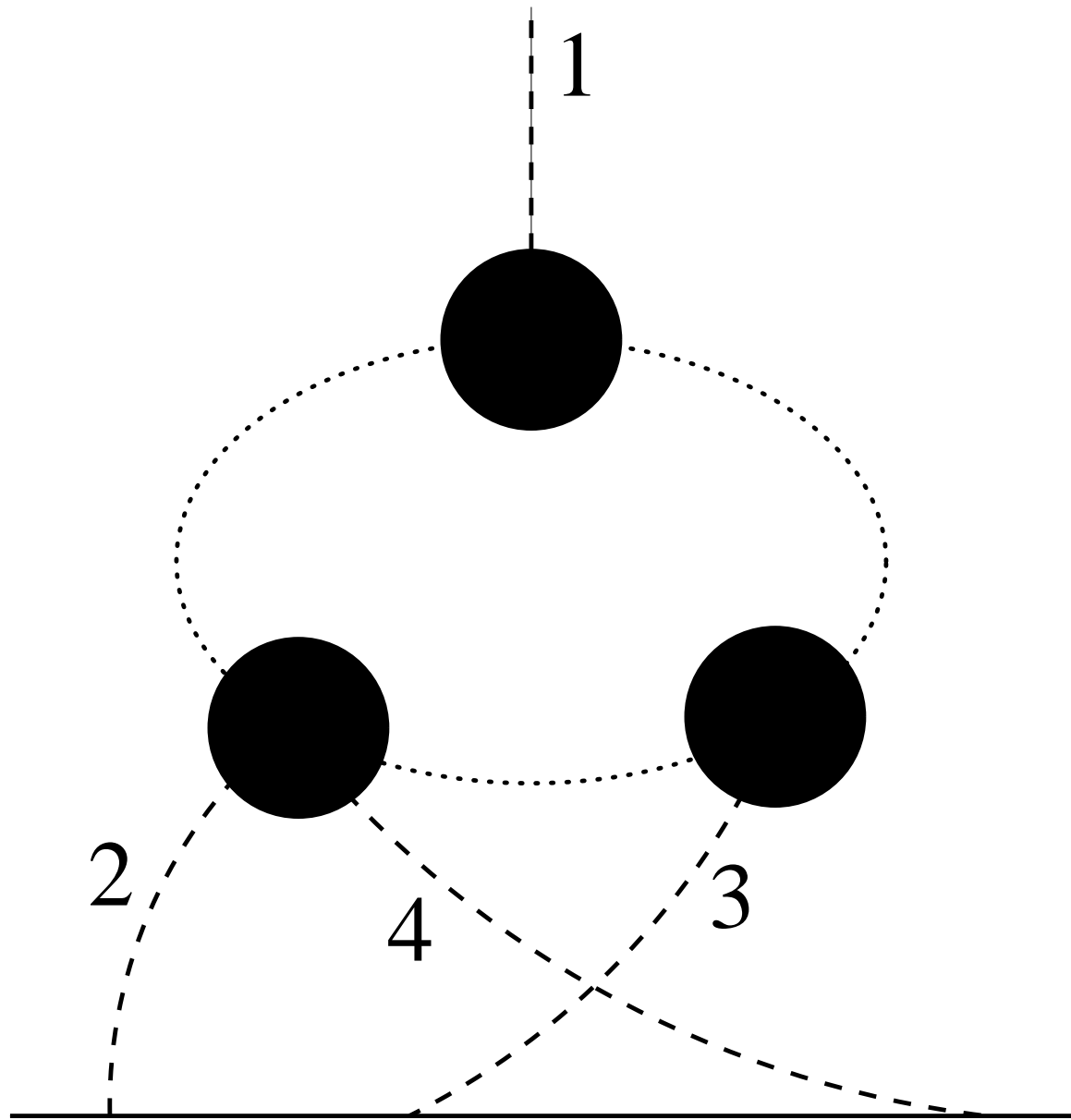


FIG. 4